



## An Explicit and Highly Accurate Runge-Kutta Family

Rezaiee-Pajand, M.<sup>1\*</sup> , Esfehni, S.A.H.<sup>2</sup> and Ehsanmanesh, H.<sup>3</sup>

<sup>1</sup> Professor, Civil Engineering Department, Faculty of Engineering, Ferdowsi University of Mashhad, Mashhad, Iran.

<sup>2</sup> M.Sc., Civil Engineering Department, Faculty of Engineering, Ferdowsi University of Mashhad, Mashhad, Iran.

<sup>3</sup> B.Sc., Department of Electrical Engineering, Faculty of Engineering, Ferdowsi University of Mashhad, Mashhad, Iran.

© University of Tehran 2022

Received: 16 Sep. 2021;

Revised: 14 May 2022;

Accepted: 17 Jul. 2022

**ABSTRACT:** In this paper, an explicit family with higher-order of accuracy is proposed for dynamic analysis of structural and mechanical systems. By expanding the analytical amplification matrix into Taylor series, the Runge-Kutta family with  $n$  stages can be presented. The required coefficients ( $\alpha$ ) for different stages are calculated through a solution of nonlinear algebraic equations. The contribution of the new family is the equality between its accuracy order, and the number of stages used in a single time step ( $n$ ). As a weak point, the stability of the proposed family is conditional, so that the stability domain for each of the first three orders ( $n = 5, 6, \text{ and } 7$ ) is smaller than that for the classic fourth-order Runge-Kutta method. However, as a positive point, the accuracy of the family boosts as the order of the family increases. As another positive point, any arbitrary order of the family can be easily achieved by solving the nonlinear algebraic equations. The robustness and ability of the authors' schemes are illustrated over several useful time integration methods, such as Newmark linear acceleration, generalized- $\alpha$ , and explicit and implicit Runge-Kutta methods. Moreover, various numerical experiments are utilized to show higher performances of the explicit family over the other methods in accuracy and computation time. The results demonstrate the capability of the new family in analyzing nonlinear systems with many degrees of freedom. Further to this, the proposed family achieves accurate results in analyzing tall building structures, even if the structures are under realistic loads, such as ground motion loads.

**Keywords:** Accuracy, Linear and Nonlinear Dynamic Systems, Stability, Tall Building Structure, Taylor Series.

### 1. Introduction

The ability of structural analysis can be regarded as one of the most important achievements on the engineering field (Haj Najafi and Tehranizadeh, 2016; Ghassemieh and Badrkhani Ajaei, 2018;

Ezoddin et al., 2020; Kordi and Mahmoudi, 2022). Time integration methods offer numerous techniques to analyze structural and mechanical dynamic systems with high efficiency (Bathe, 1982; Goel et al., 2018; Rezaie et al., 2018). These techniques are implemented to calculate the dynamic

\* Corresponding author E-mail: mrpajand@yahoo.com

responses of the motion in linear and nonlinear systems (Chang, 2013; Soares and Großholz, 2018). It is well-known that Newmark's paper in 1959 is considered as one of the fundamental works in this scope (Newmark, 1959).

In time integration methods, time is divided into several time steps (Shutov et al., 2013), in which the length of time steps might be equal or different (Rossi et al., 2014). Time integration methods are typically classified as explicit or implicit. In explicit algorithms, the response at the end of each step is directly calculated based on the initial value of the response, as well as, the initial and current values of inputs (Kim, 2019). Some researchers developed their methods based on this idea (Hulbert and Chung, 1996; Soares, 2016). On the other hand, in implicit schemes, the response at the end of each time step not only depends on its initial value, but also on the response value at the end of the time step (Lee et al., 2017). In this manner, the response is usually obtained by solving an algebraic equation. Many researchers proposed various implicit time integrations to solve linear and nonlinear dynamic systems (Newmark, 1959; Ortigosa et al., 2020). By combining the explicit and implicit schemes, predictor-corrector methods have been developed. In these procedures, an explicit algorithm is deployed to approximate the initial solution of the response. In the next step, an implicit method is utilized to modify the obtained solution (Noels et al., 2006; Yaghoubi et al., 2016).

A large group of methods, known as Runge-Kutta schemes and their derivations, has been developed over decades to deal with dynamic equations. The first useful group is known as 2<sup>nd</sup>-order and 4<sup>th</sup>-order Runge-Kutta schemes, which were introduced by Heun (1900) and Kutta (1901), respectively. Thereafter, different methods have been proposed based on Runge-Kutta techniques (Izzo and Jackiewicz, 2017; Jørgensen et al., 2018). It is worth emphasizing that some of these

methods are explicit, and some others are based on implicit techniques (Zhao and Wei, 2014; Grote et al., 2015). More to this, some researchers presented predictor-corrector Runge-Kutta algorithms (Gu and Zhu, 2021). Butcher (2016) proposed a general table to illustrate the majority of the Runge-Kutta schemes. Each Runge-Kutta method exploits a number of stages to achieve the response at the end of time step. The accuracy order of the scheme will be improved by increasing the number of stages. However, based on the results of Butcher's study, in order to achieve an accuracy order greater than 4 in an explicit Runge-Kutta scheme, the number of utilized stages should be larger than the desired accuracy order (Hairer et al., 2006). Fok (2016) proposed a 4<sup>th</sup>-order of accuracy Runge-Kutta method. In his scheme, the length of time step is changed to control the error of response solution. Braš et al. (2017) suggested an explicit-implicit method to obtain a Runge-Kutta family with various orders of accuracy, from the first- to the fourth-order. In their technique, the number of stages is equal to the accuracy order of the method. Grote et al. (2015) proposed some explicit forms of the local time-stepping Runge-Kutta method up to the 4<sup>th</sup>-order. Based on Runge-Kutta techniques, Zhao and Wei (2014) developed a new discrete Galerkin method for time integration. The highest order of accuracy provided by this approach, which is an implicit Runge-Kutta technique, is equal to 6. Many scholars offered some methods in which their order of accuracy varies between 1 and 5 (Izzo and Jackiewicz, 2017; Isherwood et al., 2018; Jørgensen et al., 2018; Martín-Vaquero and Kleefeld, 2019). However, some of the proposed procedures have a higher order of accuracy, which can only solve free vibration problems (Turaci and Öziş, 2018; Sun and Shu, 2019).

Some researchers use the expansion of the exponential matrix to develop their Runge-Kutta family. For example, Vejju et al. (2016) computed the state transition

matrix using Lagrange's interpolation formula for the general solution of linear dynamical systems. In their method, the exponential of a matrix is approximated by Lagrange's interpolation polynomials. However, the coefficients required for Lagrange's interpolation should be calculated for every dynamic system. Kassam and Trefethen (2005) proposed a modified exponential time difference fourth-order Runge-Kutta method to solve stiff nonlinear PDEs. Based on the experiments performed, the maximum order of accuracy of their method is 5. Zhang et al. (2020) invented an exponential Runge-Kutta method with second-order accuracy in space and fourth-order accuracy in time. In their algorithm, the product of a block Toeplitz matrix exponential and a vector is calculated by the shift-invert Lanczos method. A survey on the literature manifests that researchers have carried out a great deal of work concerning the dynamic analysis of structures. So far, various strategies have been proposed to increase the order of accuracy and stability of different methods. Nonetheless, the development of a family capable of furnishing any arbitrary order remains a significant challenge.

This paper presents a comprehensive explicit family of Runge-Kutta methods to deal with linear and nonlinear structural dynamic systems. In this manner, the amplification matrix of analytical solution is expanded into Taylor series, and by solving a system of nonlinear algebraic equations, coefficients required ( $\alpha$ ) for the stages of the Runge-Kutta family are obtained. One of the superiorities of the proposed formulation is the equality between the method accuracy order, and the number of stages used in a single time step. Aside from this, any arbitrary order of the family can be easily achieved by solving a system of algebraic equations.

## 2. Proposed Scheme

### 2.1. Linear Dynamic Systems

In linear structural dynamics, the

equation of motion with initial values for displacement ( $\mathbf{u}_0$ ) and velocity ( $\dot{\mathbf{u}}_0$ ) is written in the following form.

$$\begin{aligned} \mathbf{M}\ddot{\mathbf{u}}(t) + \mathbf{C}\dot{\mathbf{u}}(t) + \mathbf{K}\mathbf{u}(t) &= \mathbf{f}(t) \\ \mathbf{u}(0) = \mathbf{u}_0, \dot{\mathbf{u}}(0) &= \dot{\mathbf{u}}_0 \end{aligned} \quad (1)$$

where,  $\mathbf{M}$ ,  $\mathbf{C}$ , and  $\mathbf{K}$ : are the mass, damping, and linear stiffness matrices of the structure, respectively. Also,  $\mathbf{u}$ ,  $\dot{\mathbf{u}}$ ,  $\ddot{\mathbf{u}}$  and  $\mathbf{f}$ : are vectors showing the displacement, velocity, acceleration, and applied loads in different nodes of the structure at time  $t$ , respectively. Eq. (1) can be formulated in the form of state-space representation as follows:

$$\dot{\mathbf{x}} = \mathbf{M} \mathbf{x} + \mathbf{p} \quad (2)$$

in which,  $\mathbf{x}$ : is the state space vector of Eq. (2) and is given by:

$$\mathbf{x} = \begin{Bmatrix} \mathbf{u} \\ \dot{\mathbf{u}} \end{Bmatrix} \quad (3)$$

where,  $\dot{\mathbf{x}}$ ,  $\mathbf{p}$ , and  $\mathbf{M}$ : are derivative of the state vector, input vector, and state coefficient matrix, respectively. The input vector  $\mathbf{p}$  and state coefficient matrix  $\mathbf{M}$  are expressed as follows.

$$\mathbf{p} = \begin{Bmatrix} \mathbf{0}_{k \times 1} \\ \mathbf{M}^{-1}\mathbf{f}(t) \end{Bmatrix} \quad (4)$$

$$\mathbf{M} = \begin{bmatrix} \mathbf{0}_{k \times k} & \mathbf{I}_{k \times k} \\ -\mathbf{M}^{-1}\mathbf{K} & -\mathbf{M}^{-1}\mathbf{C} \end{bmatrix} \quad (5)$$

where,  $\mathbf{0}_{k \times k}$  and  $\mathbf{I}_{k \times k}$ : represent zero and identity matrices, respectively, and  $k$ : shows the degrees of freedom for the structure with the equation of motion in Eq. (1). In the time integration process, the time-domain  $[0, t]$  is divided into  $m$  subdomains, each having a length of  $\Delta t$ . These are called time steps. At each step, the values provided at the beginning of the step, and the input vector are used to calculate the responses at the end of the step. The value of the input vector at each step is defined as follows:

$$\mathbf{p}_i(\tau) = \mathbf{p}((i-1)\Delta t + \tau); \quad 0 \leq \tau \leq \Delta t \quad (6)$$

where,  $i$ : shows the step number and  $\tau$ : is a

time variable that varies in  $[0, \Delta t]$ . The exact solution of Eq. (2) at the end of the time step  $i$  is achievable as follows:

$$\mathbf{x}_{i+1} = e^{\mathbf{M} \Delta t} \mathbf{x}_i + \int_0^{\Delta t} e^{\mathbf{M} \tau} \mathbf{p}_i(\Delta t - \tau) d\tau \quad (7)$$

where  $\mathbf{x}_i$  and  $\mathbf{x}_{i+1}$ : represent the initial and final values of the solution of Eq. (2) at  $i$ th time step. Taylor series expansion for the exponential matrix functions given in Eq. (7) (i.e.  $e^{\mathbf{M} \Delta t}$  and  $e^{\mathbf{M} \tau}$ ) can be represented in the following equations:

$$e^{\mathbf{M} \Delta t} = \mathbf{I} + \frac{\mathbf{M} \Delta t}{1!} + \frac{\mathbf{M}^2 \Delta t^2}{2!} + \frac{\mathbf{M}^3 \Delta t^3}{3!} + \dots + \frac{\mathbf{M}^n \Delta t^n}{n!} + \dots = \mathbf{I} + \sum_{s=1}^{\infty} \frac{\mathbf{M}^s \Delta t^s}{s!} \quad (8)$$

$$e^{\mathbf{M} \tau} = \mathbf{I} + \frac{\mathbf{M} \tau}{1!} + \frac{\mathbf{M}^2 \tau^2}{2!} + \frac{\mathbf{M}^3 \tau^3}{3!} + \dots + \frac{\mathbf{M}^n \tau^n}{n!} + \dots = \mathbf{I} + \sum_{s=1}^{\infty} \frac{\mathbf{M}^s \tau^s}{s!} \quad (9)$$

By substituting Eqs. (8) and (9) into Eq. (7), the exact solution of Eq. (2) at the  $i$ th step is rewritten in the below form:

$$\mathbf{x}_{i+1} = \left( \mathbf{I} + \sum_{s=1}^{\infty} \frac{\mathbf{M}^s \Delta t^s}{s!} \right) \mathbf{x}_i + \int_0^{\Delta t} \left( \mathbf{I} + \sum_{s=1}^{\infty} \frac{\mathbf{M}^s \tau^s}{s!} \right) \mathbf{p}_i(\Delta t - \tau) d\tau \quad (10)$$

Similar to other Runge-Kutta schemes, the proposed formulation uses the initial value  $\mathbf{X}_i$  to produce the increments of the variable  $\mathbf{X}$  ( $\Delta \mathbf{X}$ ) in some stages. In this manner, the increments are calculated as follows:

$$\begin{aligned} \mathbf{X}_0 &= \mathbf{x}_i \\ \mathbf{X}_1 &= \mathbf{X}_0 \\ \Delta \mathbf{X}_1 &= \mathcal{M}(\mathbf{X}_1 + \mathbf{P}_1) \Delta t \\ \mathbf{X}_2 &= \mathbf{X}_0 + \alpha_1 \Delta \mathbf{X}_1 \\ \Delta \mathbf{X}_2 &= \mathcal{M}(\mathbf{X}_2 + \mathbf{P}_2) \Delta t \\ \mathbf{X}_3 &= \mathbf{X}_0 + \alpha_2 \Delta \mathbf{X}_2 \\ \Delta \mathbf{X}_3 &= \mathcal{M}(\mathbf{X}_3 + \mathbf{P}_3) \Delta t \\ &\dots \\ \mathbf{X}_{n-1} &= \mathbf{X}_0 + \alpha_{n-2} \Delta \mathbf{X}_{n-2} \\ \Delta \mathbf{X}_{n-1} &= \mathcal{M}(\mathbf{X}_{n-1} + \mathbf{P}_{n-1}) \Delta t \\ \mathbf{X}_n &= \mathbf{X}_0 + \alpha_{n-1} \Delta \mathbf{X}_{n-1} \\ \Delta \mathbf{X}_n &= \mathcal{M}(\mathbf{X}_n + \mathbf{P}_n) \Delta t \end{aligned} \quad (11)$$

where  $n$ : denotes the number of the utilized stages. Eventually, using the initial values and weighted average of the increments ( $\Delta \mathbf{X}$ ), the responses at the end of the time step  $i$  is achievable by using Eq. (12).

$$\mathbf{x}_{i+1} = \mathbf{X}_0 + \mathbf{P}_0 + \frac{\Delta \mathbf{X}_1 + \frac{1}{\alpha_1} \Delta \mathbf{X}_2 + \dots + \frac{1}{\alpha_{n-1}} \Delta \mathbf{X}_n}{1 + \frac{1}{\alpha_1} + \frac{1}{\alpha_2} + \dots + \frac{1}{\alpha_{n-1}}} \quad (12)$$

in which coefficients  $\alpha_1$  to  $\alpha_{n-1}$  and vectors  $\mathbf{P}_0$  to  $\mathbf{P}_n$ : represent the unknown quantities, which should be calculated. By using Eqs. (11) and (12), Eq. (13) is achieved.

$$\mathbf{x}_{i+1} = \mathbf{x}_i + \mathbf{P}_0 + \left( 1 + \sum_{j=1}^{n-1} \frac{1}{\alpha_j} \right)^{-1} \mathbf{X} \mathbf{P} \quad (13)$$

where,  $\mathbf{X} \mathbf{P}$  is defined as follows.

$$\begin{aligned} \mathbf{X} \mathbf{P} &= \left( 1 + \sum_{j=1}^{n-1} \frac{1}{\alpha_j} \right) \mathbf{M} \Delta t + [n-1] \mathbf{M}^2 \Delta t^2 + \\ &\left[ \sum_{j=1}^{n-2} \alpha_j \right] \mathbf{M}^3 \Delta t^3 + \left[ \sum_{j=1}^{n-3} \alpha_j \alpha_{j+1} \right] \mathbf{M}^4 \Delta t^4 + \\ &\left[ \sum_{j=1}^{n-4} \alpha_j \alpha_{j+1} \alpha_{j+2} \right] \mathbf{M}^5 \Delta t^5 + \\ &\left[ \sum_{j=1}^{n-5} \prod_{v=0}^3 \alpha_{j+v} \right] \mathbf{M}^6 \Delta t^6 + \dots + \left[ \prod_{v=1}^{n-2} \alpha_v \right] \mathbf{M}^n \Delta t^n \mathbf{x}_i \\ &+ (\mathbf{M} \Delta t [\mathbf{P}_1 + \frac{1}{\alpha_1} \mathbf{P}_2 + \frac{1}{\alpha_2} \mathbf{P}_3 \\ &+ \dots + \frac{1}{\alpha_{n-2}} \mathbf{P}_{n-1} + \frac{1}{\alpha_{n-1}} \mathbf{P}_n] \\ &+ \mathbf{M}^2 \Delta t^2 [\mathbf{P}_1 + \mathbf{P}_2 + \mathbf{P}_3 + \dots + \mathbf{P}_{n-2} + \mathbf{P}_{n-1}] \\ &+ \mathbf{M}^3 \Delta t^3 [\alpha_1 \mathbf{P}_1 + \alpha_2 \mathbf{P}_2 + \dots + \alpha_{n-2} \mathbf{P}_{n-2}] \\ &+ \mathbf{M}^4 \Delta t^4 [\alpha_1 \alpha_2 \mathbf{P}_1 + \alpha_2 \alpha_3 \mathbf{P}_2 + \alpha_3 \alpha_4 \mathbf{P}_3 \\ &+ \dots + \alpha_{n-4} \alpha_{n-3} \mathbf{P}_{n-4} + \alpha_{n-3} \alpha_{n-2} \mathbf{P}_{n-3}] \\ &+ \dots \\ &+ \mathbf{M}^{k+1} \Delta t^{k+1} [\alpha_1 \dots \alpha_{k-1} \mathbf{P}_1 + \alpha_2 \dots \alpha_k \mathbf{P}_2 \\ &+ \dots + \alpha_{n-k} \dots \alpha_{n-2} \mathbf{P}_{n-k}] \\ &+ \mathbf{M}^{n-1} \Delta t^{n-1} [\alpha_1 \dots \alpha_{n-3} \mathbf{P}_1 + \alpha_2 \dots \alpha_{n-2} \mathbf{P}_2] \\ &+ \mathbf{M}^n \Delta t^n [\alpha_1 \dots \alpha_{n-2} \mathbf{P}_1] \end{aligned} \quad (14)$$

By substituting Eq. (14) into Eq. (13), Eq. (13) can be expanded in the following form.

$$\begin{aligned} \mathbf{x}_{i+1} &= \left(\mathbf{I} + \left(1 + \sum_{j=1}^{n-1} \frac{1}{\alpha_j}\right)\right)^{-1} \left[\left(1 + \sum_{j=1}^{n-1} \frac{1}{\alpha_j}\right) \mathbf{M} \Delta t \right. \\ &+ (n-1) \mathbf{M}^2 \Delta t^2 + \dots + \left. \prod_{v=1}^{n-2} \alpha_v \mathbf{M}^n \Delta t^n\right] \mathbf{x}_i \\ &+ \left(\mathbf{P}_0 + \left(1 + \sum_{j=1}^{n-1} \frac{1}{\alpha_j}\right)^{-1} \right. \\ &\left. \left[\mathbf{M} \Delta t \left[\mathbf{P}_1 + \frac{1}{\alpha_1} \mathbf{P}_2 + \dots + \frac{1}{\alpha_{n-1}} \mathbf{P}_n\right] \right. \right. \\ &\left. \left. + \dots + \mathbf{M}^n \Delta t^n [\alpha_1 \dots \alpha_{n-2} \mathbf{P}_1]\right]\right) \end{aligned} \tag{15}$$

According to Eq. (10), if the number of selected terms in the series is limited to  $n$ , one can arrive at:

$$\begin{aligned} \mathbf{x}_{i+1} &= \left(\mathbf{I} + \sum_{s=1}^n \frac{\mathbf{M}^s \Delta t^s}{s!}\right) \mathbf{x}_i + \\ &\int_0^{\Delta t} \left(\mathbf{I} + \sum_{s=1}^n \frac{\mathbf{M}^s \tau^s}{s!}\right) \mathbf{p}_i (\Delta t - \tau) d\tau \end{aligned} \tag{16}$$

Both Eqs. (15) and (16) consist of two parts corresponding to the initial value and the input vector at the time step  $i$ . By equating the part which is associated with the initial value of the step  $i$  in Eqs. (15) and (16), one can write:

$$\begin{aligned} &\mathbf{I} + \left(1 + \sum_{j=1}^{n-1} \frac{1}{\alpha_j}\right)^{-1} \left[\left(1 + \sum_{j=1}^{n-1} \frac{1}{\alpha_j}\right) \mathbf{M} \Delta t + \right. \\ &(n-1) \mathbf{M}^2 \Delta t^2 + \dots + \left. \prod_{v=1}^{n-2} \alpha_v \mathbf{M}^n \Delta t^n\right] \tag{17} \\ &= \mathbf{I} + \sum_{s=1}^n \frac{\mathbf{M}^s \Delta t^s}{s!} \end{aligned}$$

According to Eq. (17), the required relations for obtaining the unknown coefficients,  $\alpha_1$  to  $\alpha_{n-1}$ , are as follows.

$$\begin{aligned} &\frac{1 + \sum_{j=1}^{n-1} \frac{1}{\alpha_j}}{1 + \sum_{j=1}^{n-1} \frac{1}{\alpha_j}} = \frac{1}{1!} \\ &\frac{n-1}{1 + \sum_{j=1}^{n-1} \frac{1}{\alpha_j}} = \frac{1}{2!} \\ &\frac{\sum_{j=1}^{n-2} \alpha_j}{1 + \sum_{j=1}^{n-1} \frac{1}{\alpha_j}} = \frac{1}{3!} \\ &\frac{\sum_{j=1}^{n-3} \alpha_j \alpha_{j+1}}{1 + \sum_{j=1}^{n-1} \frac{1}{\alpha_j}} = \frac{1}{4!} \\ &\dots \\ &\frac{\sum_{j=1}^{n-(k-1)} \prod_{v=0}^{k-3} \alpha_{j+v}}{1 + \sum_{j=1}^{n-1} \frac{1}{\alpha_j}} = \frac{1}{k!} \\ &\dots \\ &\frac{\prod_{v=1}^{n-2} \alpha_v}{1 + \sum_{j=1}^{n-1} \frac{1}{\alpha_j}} = \frac{1}{n!} \end{aligned} \tag{18}$$

It is obvious that the values of all coefficients,  $\alpha_1$  to  $\alpha_{n-1}$ , for any arbitrary  $n$ , can be available. The studies about the uniqueness and existence of the coefficients  $\alpha_1$  to  $\alpha_{n-1}$  are presented in Appendix 1. These coefficients are outlined in Table 1 for  $n$  from 2 to 10. To obtain the unknown vectors of  $\mathbf{P}_0$  to  $\mathbf{P}_n$ , the part of Eqs. (15) and (16) concerned with the input vector must be equated. In this manner, the corresponding equality can be expressed as:

$$\begin{aligned} &\mathbf{P}_0 + \left(1 + \sum_{j=1}^{n-1} \frac{1}{\alpha_j}\right)^{-1} \\ &\left[\mathbf{M} \Delta t \left[\mathbf{P}_1 + \frac{1}{\alpha_1} \mathbf{P}_2 + \dots + \frac{1}{\alpha_{n-1}} \mathbf{P}_n\right] \right. \\ &\left. + \dots + \mathbf{M}^n \Delta t^n [\alpha_1 \dots \alpha_{n-2} \mathbf{P}_1]\right] \tag{19} \\ &= \int_0^{\Delta t} \left(\mathbf{I} + \sum_{s=1}^n \frac{\mathbf{M}^s \tau^s}{s!}\right) \mathbf{p}_i (\Delta t - \tau) d\tau \end{aligned}$$

From Eq. (18), one can find out that the term  $\left(1 + \sum_{j=1}^{n-1} \frac{1}{\alpha_j}\right)$  is equal to  $2(n-1)$ . Using this equality and according to Eq. (19), one can use the equalities provided in Eq. (20) to calculate the unknown vectors  $\mathbf{P}_0$  to  $\mathbf{P}_n$ .

**Table 1.** Values of coefficients  $\alpha_{(1 \text{ to } n-1)}$  for  $n = 2$  to 10

$n$	$\alpha_{(1 \text{ to } n-1)}$
2	$\alpha_1 = 1$
3	$\alpha_1 = \frac{2}{3}, \alpha_2 = \frac{2}{3}$
4	$\alpha_1 = \frac{1}{2}, \alpha_2 = \frac{1}{2}, \alpha_3 = 1$
5	$\alpha_1 = 0.276393202250021, \alpha_2 = \frac{1}{3}, \alpha_3 = 0.723606797749979, \alpha_4 = -1$
6	$\alpha_1 = 0.204201653860479, \alpha_2 = 0.230959413182896,$ $\alpha_3 = 0.324788653084487, \alpha_4 = 0.906716946538805,$ $\alpha_5 = -0.226824729490652$
7	$\alpha_1 = 0.164001419299363, \alpha_2 = 0.180945030752080,$ $\alpha_3 = 0.224567849422043, \alpha_4 = 0.322442384424107,$ $\alpha_5 = 1.108043316102407, \alpha_6 = -0.110121647194359$
8	$\alpha_1 = 0.138024395659493, \alpha_2 = 0.150377394128368,$ $\alpha_3 = 0.177126116082260, \alpha_4 = 0.222065352065870,$ $\alpha_5 = 0.321068289581217, \alpha_6 = 1.324671785816124,$ $\alpha_7 = 1.324671785816124$
9	$\alpha_1 = 0.119669128822673, \alpha_2 = 0.129338229567660,$ $\alpha_3 = 0.148026233263177, \alpha_4 = 0.175655856970635,$ $\alpha_5 = 0.220533539633299, \alpha_6 = 0.319746278224780,$ $\alpha_7 = 1.553697400184442, \alpha_8 = -0.045783116925874$
10	$\alpha_1 = 0.105907195963393, \alpha_2 = 0.113787598394926,$ $\alpha_3 = 0.127824138883028, \alpha_4 = 0.147160952467405,$ $\alpha_5 = 0.174797828444654, \alpha_6 = 0.219349289937336,$ $\alpha_7 = 0.318322435005099, \alpha_8 = 1.792850560904159,$ $\alpha_9 = -0.033525393846740$

$$\begin{aligned}
\mathbf{P}_0 &= \int_0^{\Delta t} \mathbf{p}_i (\Delta t - \tau) d\tau \\
\frac{1}{2(n-1)} \mathbf{M} \Delta t (\mathbf{P}_1 + \frac{1}{\alpha_1} \mathbf{P}_2 + \frac{1}{\alpha_2} \mathbf{P}_3 + \dots \\
&+ \frac{1}{\alpha_{n-1}} \mathbf{P}_n) = \frac{\mathbf{M}}{1!} \int_0^{\Delta t} \tau \mathbf{p}_i (\Delta t - \tau) d\tau \\
\frac{1}{2(n-1)} \mathbf{M}^2 \Delta t^2 (\mathbf{P}_1 + \mathbf{P}_2 + \mathbf{P}_3 + \dots + \mathbf{P}_{n-1}) &= \\
\frac{\mathbf{M}^2}{2!} \int_0^{\Delta t} \tau^2 \mathbf{p}_i (\Delta t - \tau) d\tau & \quad (20) \\
\frac{1}{2(n-1)} \mathbf{M}^3 \Delta t^3 (\alpha_1 \mathbf{P}_1 + \alpha_2 \mathbf{P}_2 + \alpha_3 \mathbf{P}_3 + \dots \\
&+ \alpha_{n-2} \mathbf{P}_{n-2}) = \frac{\mathbf{M}^3}{3!} \int_0^{\Delta t} \tau^3 \mathbf{p}_i (\Delta t - \tau) d\tau \\
&\dots \\
\frac{1}{2(n-1)} \mathbf{M}^n \Delta t^n (\alpha_1 \alpha_2 \alpha_3 \dots \alpha_{n-2} \mathbf{P}_1) &= \\
\frac{\mathbf{M}^n}{n!} \int_0^{\Delta t} \tau^n \mathbf{p}_i (\Delta t - \tau) d\tau &
\end{aligned}$$

It would be cumbersome and rather

impossible in some cases to calculate the above integrations in a general form. In order to reduce the complexity and make the solution straightforward, the Taylor series expansion of the term  $\mathbf{p}_i (\Delta t - \tau)$  given in the following form can be utilized.

$$\begin{aligned}
\mathbf{p}_i (\Delta t - \tau) &\approx \mathbf{p}_i (0) + \frac{\dot{\mathbf{p}}_i (0)}{1!} (\Delta t - \tau) + \\
&\frac{\ddot{\mathbf{p}}_i (0)}{2!} (\Delta t - \tau)^2 + \dots + \frac{\mathbf{p}_i^{(n)} (0)}{n!} (\Delta t - \tau)^n & (21)
\end{aligned}$$

By substituting Eq. (21) into Eq. (20), the unknown vectors  $\mathbf{P}_0$  to  $\mathbf{P}_n$  will be achieved.

## 2.2. Nonlinear Dynamic Systems

The general form of a nonlinear dynamic equation is as follows:

$$M\ddot{\mathbf{u}}(t) + \mathbf{F}(\mathbf{u}(t), \dot{\mathbf{u}}(t)) = \mathbf{f}(t) \quad (22)$$

The relation between  $\ddot{\mathbf{u}}(t)$  and  $\mathbf{u}(t)$ ,  $\dot{\mathbf{u}}(t)$ , and  $\mathbf{f}(t)$ , can be expressed as:

$$\ddot{\mathbf{u}}(t) = -\mathbf{M}^{-1} \times \mathbf{F}(\mathbf{u}(t), \dot{\mathbf{u}}(t)) + \mathbf{M}^{-1} \times \mathbf{f}(t) \quad (23)$$

By considering Eq. (3), the derivative of  $\mathbf{X}$  is stated as below.

$$\dot{\mathbf{x}} = \begin{Bmatrix} \dot{\mathbf{u}}(t) \\ \ddot{\mathbf{u}}(t) \end{Bmatrix} \quad (24)$$

Based on Eqs. (23) and (24), the nonlinear dynamic system shown in Eq. (22) can be represented as Eq. (23) (Brogan, 1991).

$$\begin{aligned} \dot{\mathbf{x}} &= \begin{Bmatrix} \dot{\mathbf{u}}(t) \\ \ddot{\mathbf{u}}(t) \end{Bmatrix} \\ &= \begin{Bmatrix} \dot{\mathbf{u}}(t) \\ -\mathbf{M}^{-1} \times \mathbf{F}(\mathbf{u}(t), \dot{\mathbf{u}}(t)) + \mathbf{M}^{-1} \times \mathbf{f}(t) \end{Bmatrix} \\ &= \begin{Bmatrix} \dot{\mathbf{u}} \\ -\mathbf{M}^{-1} \times \mathbf{F}(\mathbf{u}(t), \dot{\mathbf{u}}(t)) \end{Bmatrix} + \begin{Bmatrix} 0_{k \times 1} \\ \mathbf{M}^{-1} \times \mathbf{f}(t) \end{Bmatrix} \end{aligned} \quad (25)$$

Eq. (23) has two sections that are separately

related to the state variable  $\mathbf{x} = \begin{Bmatrix} \mathbf{u}(t) \\ \dot{\mathbf{u}}(t) \end{Bmatrix}$  and

the input vector  $\mathbf{f}(t)$ . Using  $\mathbf{p}(t)$  and  $\mathbf{G}(\mathbf{x})$  presented in Eqs. (26) and (27), Eq. (25) can be rewritten in a compact form, which is shown in Eq. (28).

$$\mathbf{p}(t) = \begin{bmatrix} 0_{k \times 1} \\ \mathbf{M}^{-1} \end{bmatrix} \mathbf{f}(t) \quad (26)$$

$$\mathbf{G}(\mathbf{x}) = \mathbf{G} \left( \begin{Bmatrix} \mathbf{u} \\ \dot{\mathbf{u}} \end{Bmatrix} \right) = \begin{Bmatrix} \dot{\mathbf{u}} \\ -\mathbf{M}^{-1} \times \mathbf{F}(\mathbf{u}, \dot{\mathbf{u}}) \end{Bmatrix} \quad (27)$$

$$\dot{\mathbf{x}} = \mathbf{G}(\mathbf{x}) + \mathbf{p}(t) \quad (28)$$

Similar to the procedure explained for linear dynamic systems, in order to obtain

$\mathbf{x}_{i+1} = \begin{Bmatrix} \mathbf{u}_{i+1} \\ \dot{\mathbf{u}}_{i+1} \end{Bmatrix}$  at the time step  $i$ , the values of

$\mathbf{x}_i = \begin{Bmatrix} \mathbf{u}_i \\ \dot{\mathbf{u}}_i \end{Bmatrix}$  and  $\mathbf{P}_0$  to  $\mathbf{P}_n$  are needed. The

values of  $\mathbf{P}_0$  to  $\mathbf{P}_n$  are calculated by using  $\mathbf{p}(t)$  and through the solution of Eq. (20).

The procedure to obtain  $\mathbf{x}_{i+1}$  is shown in Figure 1.

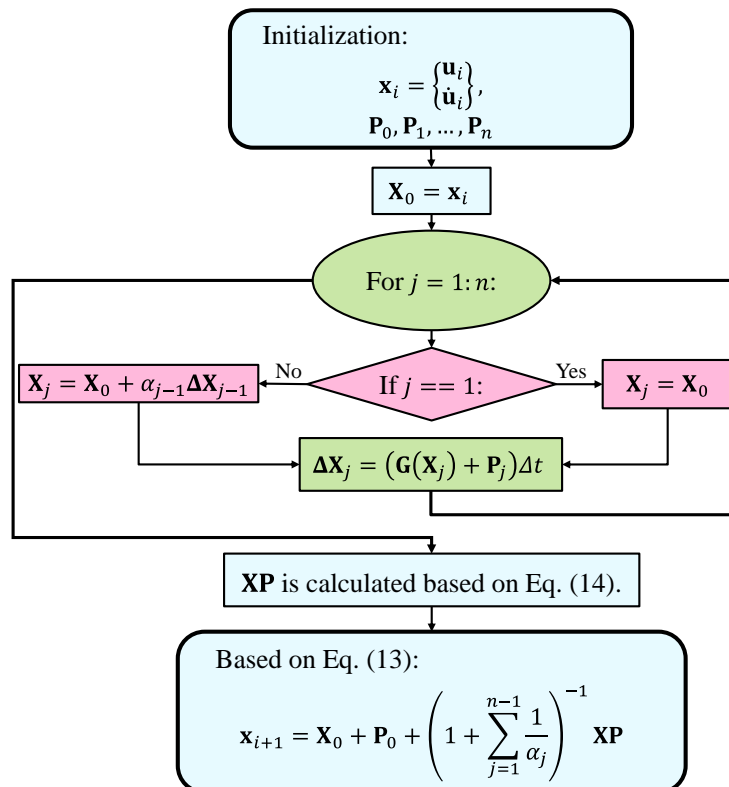


Fig. 1. The procedure for calculating  $\mathbf{x}_{i+1}$  at the time step  $i$

Based on the flowchart illustrated in Figure 1, at the beginning of the  $i$ th time step, the values of  $\mathbf{X}_i$  and  $\mathbf{P}_0$  to  $\mathbf{P}_n$  are considered. At the first,  $\mathbf{X}_0$  is set as  $\mathbf{X}_i$ . In the next step, using an iterative procedure, the increment  $\Delta\mathbf{X}_j$  is calculated for  $j = 1$  to  $n$ . In each iteration,  $\Delta\mathbf{X}_j$  is achieved by using  $\mathbf{G}(\cdot)$  function given in Eq. (27) and  $\mathbf{P}_j$  provided at the beginning of the time step  $i$ .

Finally, the value of  $\mathbf{x}_{i+1} = \begin{Bmatrix} \mathbf{u}_{i+1} \\ \dot{\mathbf{u}}_{i+1} \end{Bmatrix}$  is

achieved by using Eq. (13). Different increments of the variable  $\mathbf{X}(\Delta\mathbf{X}_j)$  are obtained explicitly and there is no recursive solution to calculate them. Also, the values of  $\mathbf{P}_0$  to  $\mathbf{P}_n$  are explicitly achieved by using Eqs. (20) and (21). Therefore, the new family can be categorized into explicit time integration groups.

### 3. Amplification Matrix

To assess the stability and numerical accuracy of the proposed method, the amplification matrix should be obtained. This matrix is calculated for a linear structure having one degree of freedom, which is shown in Eq. (29).

$$\ddot{u}(t) + 2\xi\omega\dot{u}(t) + \omega^2u(t) = 0 \quad (29)$$

where  $\omega$  and  $\xi$ : refer to the natural frequency and damping ratio of the structure, respectively. When the new scheme is applied to find the solution of the above system in the time step  $i$ , the following relationship can be presented for the solutions at the beginning and end of the time steps  $i$ :

$$\begin{Bmatrix} u_{i+1} \\ \dot{u}_{i+1} \end{Bmatrix} = \mathbf{A}(\Delta t) \begin{Bmatrix} u_i \\ \dot{u}_i \end{Bmatrix} \quad (30)$$

where  $\mathbf{A}$ : is the amplification matrix of the new method and can be presented in the following form by using Eq. (16).

$$\mathbf{A}(\Delta t) = \mathbf{I}_{2 \times 2} + \sum_{s=1}^n \frac{\mathbf{M}^s \Delta t^s}{s!} \quad (31)$$

Matrix  $\mathbf{M}$ : is the state coefficient matrix introduced in Eq. (5) and can be obtained for the system of Eq. (29) as below.

$$\mathcal{M} = \begin{bmatrix} 0_{1 \times 1} & I_{1 \times 1} \\ -(1)^{-1}(\omega^2) & -(1)^{-1}(2\xi\omega) \end{bmatrix} \quad (32)$$

$$= \begin{bmatrix} 0 & 1 \\ -\omega^2 & -2\xi\omega \end{bmatrix}$$

### 4. Numerical Stability

A method is called numerically stable if displacement and velocity at time  $t$  do not unlimitedly increase during the solution process. In a numerically stable technique, the physical conditions of the problem should not be intensified by the numerical procedures after several time steps. The stability of the proposed method is evaluated using the spectral radius of the amplification matrix. The spectral radius holds the following form for the amplification matrix  $\mathbf{A}$  obtained in Eq. (31).

$$\rho(\mathbf{A}) = \max(|\lambda_1|, |\lambda_2|) \quad (33)$$

where  $\lambda_1$  and  $\lambda_2$ : are the eigenvalues of the amplification matrix  $\mathbf{A}$ , and  $|\cdot|$ : is the absolute operator. The inequality  $\rho(\mathbf{A}) \leq 1$  must be satisfied for all values in  $\Delta t$ , to make sure that a numerical method is stable (Bathe and Wilson, 1972; Bathe, 1982; Rezaiee-Pajand et al., 2018). The spectral radius of the amplification matrix for the Newmark linear acceleration (NLA) method (Newmark, 1959), the 4<sup>th</sup>-order Runge-Kutta (RK4) technique (Kutta, 1901), and the 5<sup>th</sup>- to 7<sup>th</sup>-order of the proposed family are depicted in Figure 2. Moreover, Figure 3 presents the results for  $n = 1$  to 10 against  $\frac{\Delta t}{T}$ . In these two figures,

the damping ratio is considered to be zero. Based on Figure 2, as a weak point, the stability of the various orders of the new family is conditional. According to Figure

2, the largest stability domain belongs to NLA, RK4, and NRKF7, respectively. However, as is illustrated in Figure 3, from a general point of view, the stability domain increases by raising the value of  $n$ .

### 5. Numerical Accuracy

It is a common way that the accuracy of any time integration method is evaluated by assessing the order of accuracy, period error, and amplitude decay (Chung and Hulbert, 1993; Rezaiee-Pajand et al., 2021). The order of accuracy of the authors' scheme will be examined in Section 6. Using the eigenvalue of the amplification matrix, one can be able to evaluate the numerical errors using the following relations (Bathe, 1982; Hughes, 2012).

$$\lambda_{1,2} = \bar{a} \pm i\bar{b} = e^{(-\bar{\xi}\bar{\omega} \pm i\bar{\omega}_d)\Delta t}$$

$$\bar{\omega} = \frac{\arctan(\bar{a} / \bar{b})}{\sqrt{1 - \xi^2} \Delta t}$$

$$\bar{\omega}_d = \bar{\omega} \sqrt{1 - \xi^2}$$

$$\bar{\xi} = -\frac{\ln(\bar{a}^2 + \bar{b}^2) \sqrt{1 - \xi^2}}{2 \arctan(\bar{b} / \bar{a})}$$
(34)

in which  $\bar{\xi}$  : denotes the numerical damping ratio of a time integration method. Additionally, the numerical period can be calculated using  $\bar{T} = \frac{2\pi}{\bar{\omega}}$ . Period error is estimated by comparing  $\bar{T}$  and the true period  $T = \frac{2\pi}{\omega}$ .

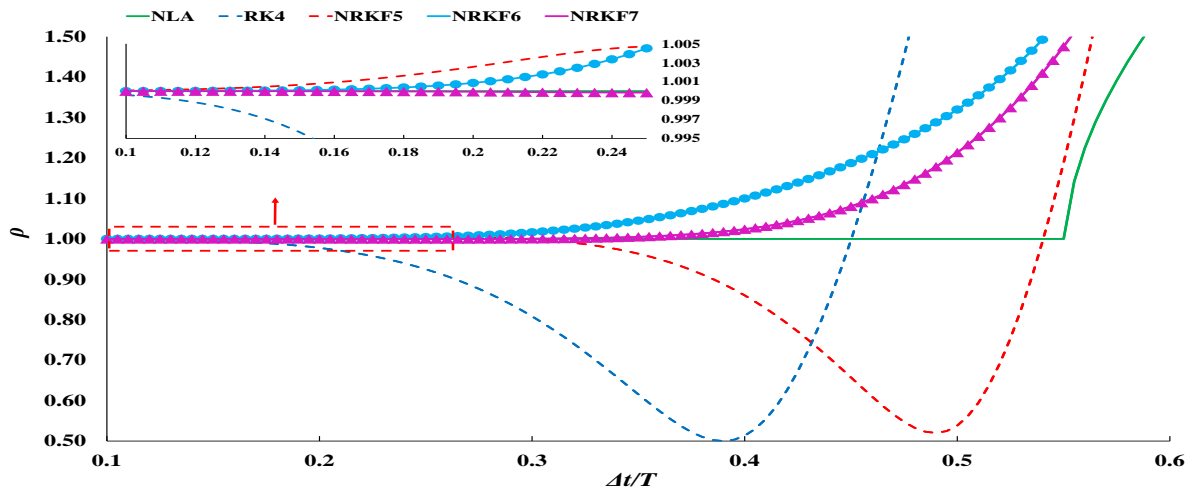


Fig. 2. The spectral radius for various schemes

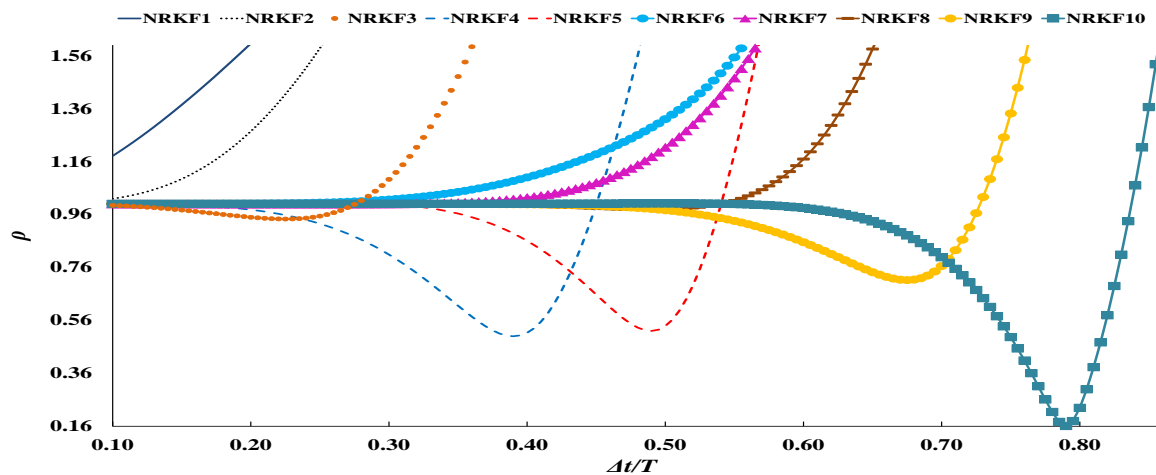


Fig. 3. The spectral radius for various orders of the new family

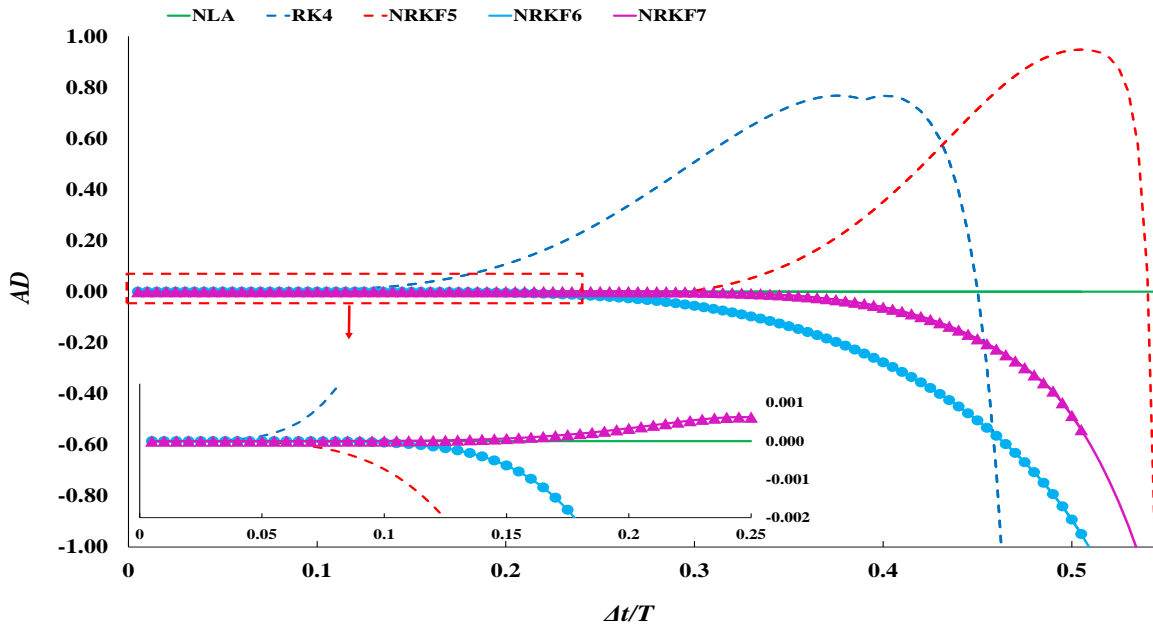


Fig. 4. Amplitude decay for various schemes

Figures 4 to 7 compare the amplitude decay and period error of the present scheme against those of the other solution techniques. Based on Figure 4, the NLA method has no elongation error, in the given domain. The proposed family method, having orders of 7, 6, and 5, and finally, the RK4 scheme possesses lower elongation errors, respectively. Figure 5 clearly indicates that an increment in the order of the presented family will lead the amplitude decay error to become nearly zero in a great interval of  $\Delta t$ .

According to the results shown in Figure 6, the nearest method in period error value to zero belongs to the proposed method with the order of 7. Then, the methods with the orders of 6 and 5, and the classic 4<sup>th</sup>-order Runge-Kutta scheme have lower values in period error, respectively. The NLA scheme has more value in period error compared to all other proposed schemes. Figure 7 displays the values of period error among different orders of the new family. As it can be observed, the value of the period error decreases as the order of the family raises.

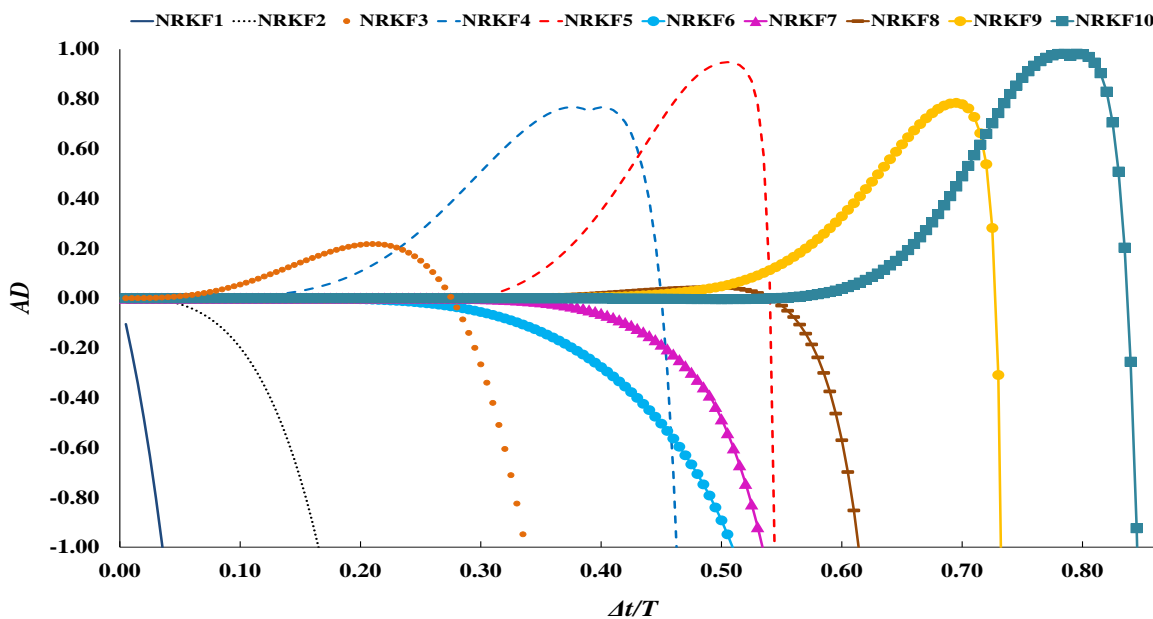


Fig. 5. Amplitude decay for various orders of the new family

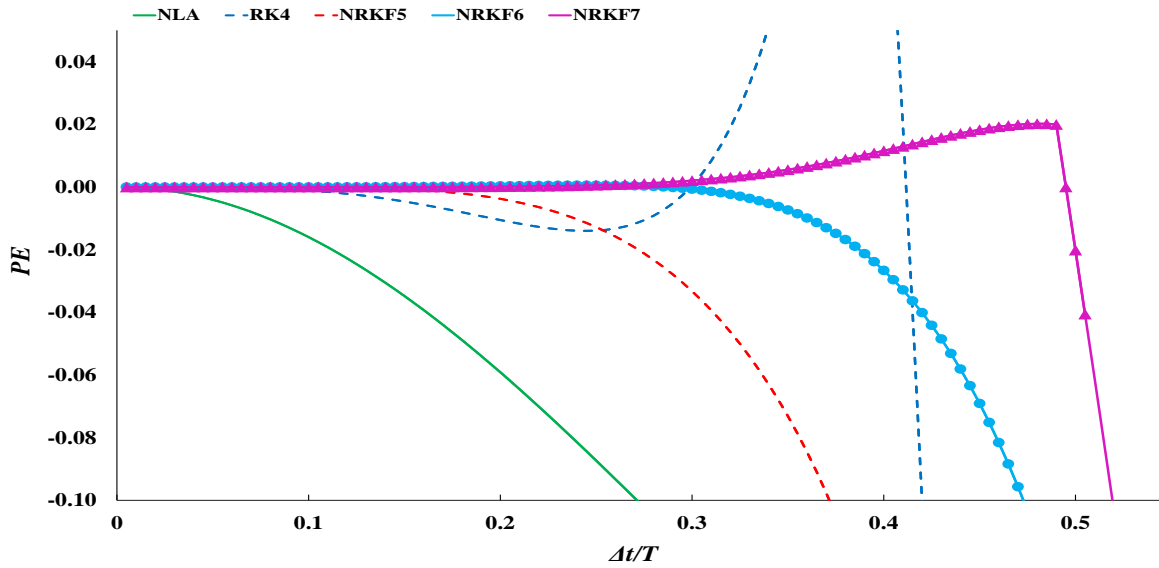


Fig. 6. Period error for various schemes

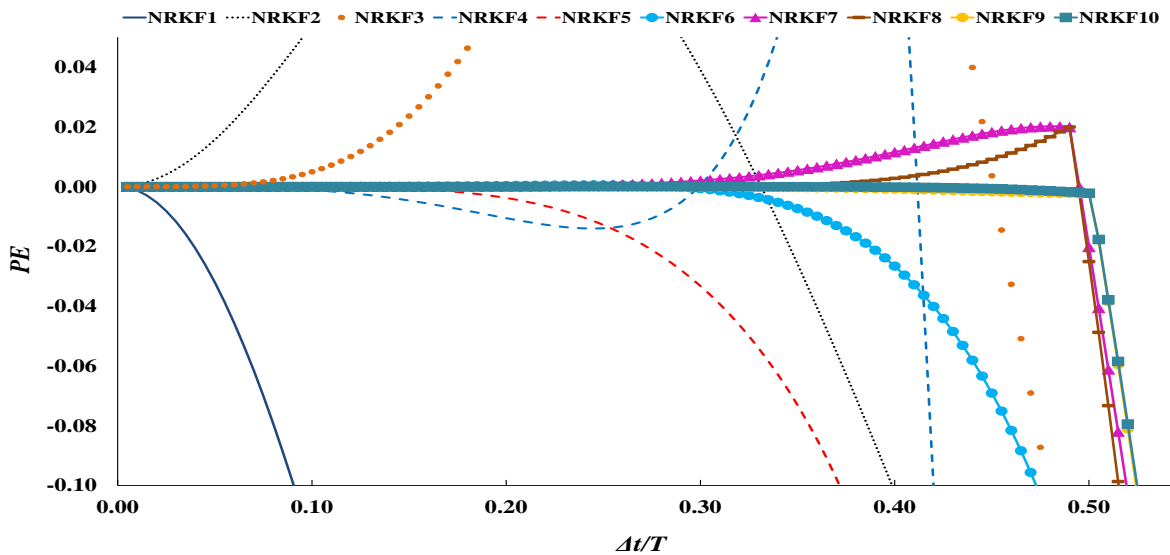


Fig. 7. Period error for various orders of the new family

### 6. Order of Accuracy

In order to determine the order of accuracy of the new time integration method, the amplification matrix of the proposed method should be compared with the analytical one (Hulbert and Hughes, 1987; Rezaiee-Pajand et al., 2021). To derive the analytical amplification matrix, the equation of motion given in Eq. (29) is considered. This equation can be changed into the subsequent equivalent first-order differential equation:

$$\dot{\mathbf{x}} = \mathbf{M} \mathbf{x} \tag{35}$$

where

$$\mathbf{x} = \begin{Bmatrix} u \\ \dot{u} \end{Bmatrix} \tag{36}$$

$$\mathbf{M} = \begin{bmatrix} 0 & 1 \\ -\omega^2 & -2\xi\omega \end{bmatrix} \tag{37}$$

The exact solution for Eq. (35) with the given initial vector  $\mathbf{x}_0 = \begin{Bmatrix} u_0 \\ \dot{u}_0 \end{Bmatrix}$  can be expressed as follows (Turyn, 2013):

$$\mathbf{x} = e^{\mathbf{M} t} \mathbf{x}_0 \tag{38}$$

Therefore, the following recursive relationship is obtained.

$$\mathbf{X}_{i+1} = e^{\mathbf{M} \Delta t} \mathbf{X}_i \quad (39)$$

The matrix  $e^{\mathbf{M} \Delta t}$ , which is the analytical amplification matrix in the equation of motion given in Eq. (29), can be expanded into Taylor series, as below (Moler and Van Loan, 2003).

$$e^{\mathbf{M} \Delta t} = \mathbf{I} + \sum_{s=1}^{\infty} \frac{\mathbf{M}^s \Delta t^s}{s!} \quad (40)$$

By comparing the Taylor series expansion of the amplification matrix outlined in Eq. (31), which belongs to the proposed family, and that in Eq. (40), it is concluded that the order of accuracy of the present family is equal to  $n$  (the order of the proposed family).

## 7. Numerical Examples

In this section, numerical examples are presented to establish the accuracy and advantages of the proposed methods. Various problems in the scope of structural and mechanical engineering, including an undamped single degree of freedom oscillator, five stories shear building with non-classic damping, a structure with two degrees of freedom subjected to impact loading, a plane truss, a three-dimensional truss, and two nonlinear systems with many degrees of freedom, are employed. The nonlinear experiments include a nonlinear mass-spring-damper system with 100 Dofs and a tall shear building structure subjected to a realistic load, the El-Centro ground motion. All linear examples are analyzed and compared through different numerical schemes, including the Newmark Linear Acceleration (NLA) technique, the 4<sup>th</sup>-order classic Runge-Kutta (RK4) scheme, an implicit 4<sup>th</sup>-order Runge-Kutta method presented by Fok (2016) (CKRK), an implicit three-step method suggested by Zhao and Wei (2014) (SRK3), and the

proposed family methods by the orders of 5, 6 and 7 (NRKF5, NRKF6, and NRKF7). The solution of the nonlinear mass-spring-damper structure is added to illustrate the capability of the new family in the analysis of nonlinear dynamic systems with many degrees of freedom. Furthermore, the example of a tall shear building structure is used to demonstrate the ability of the new family methods over broadly accepted methods such as the generalized- $\alpha$  method (Chung and Hulbert, 1993), and the higher-order implicit method, SRK3, in comparison to dealing with many degrees of freedom nonlinear structures subjected to a realistic load.

### 7.1. Undamped Single Degree of Freedom Oscillator

In the first example, the following 2<sup>nd</sup>-order differential equation is considered. It should be reminded that this equation has been widely adopted in evaluating the accuracy of several time integration schemes (Bathe, 1982; Rezaiee-Pajand et al., 2018; Rezaiee-Pajand et al., 2021).

$$\ddot{u} + u = 0 \quad (41)$$

It is assumed that the initial values of  $u_0$  and  $\dot{u}_0$  are equal to 1000 and 0, respectively. The exact solution of Eq. (41) is given by  $u_{ex} = 1000 \cos(t)$ . The time step in the numerical integration procedures is assumed as  $\Delta t = 0.1$  s and the total time of the analysis is equal to  $t = 10$  s. Figure 8 illustrates the logarithmic values of error for different methods in base 10.

According to the results demonstrated in Figure 8, the proposed family having an order of 7 gives the lowest value of error, while the NLA method possesses the highest error value. Figure 9 depicts the error values for two other techniques, the CKRK scheme and the new family method of order 5. Based on this figure, the suggested method of this paper leads to a lower error value compared to the CKRK scheme.

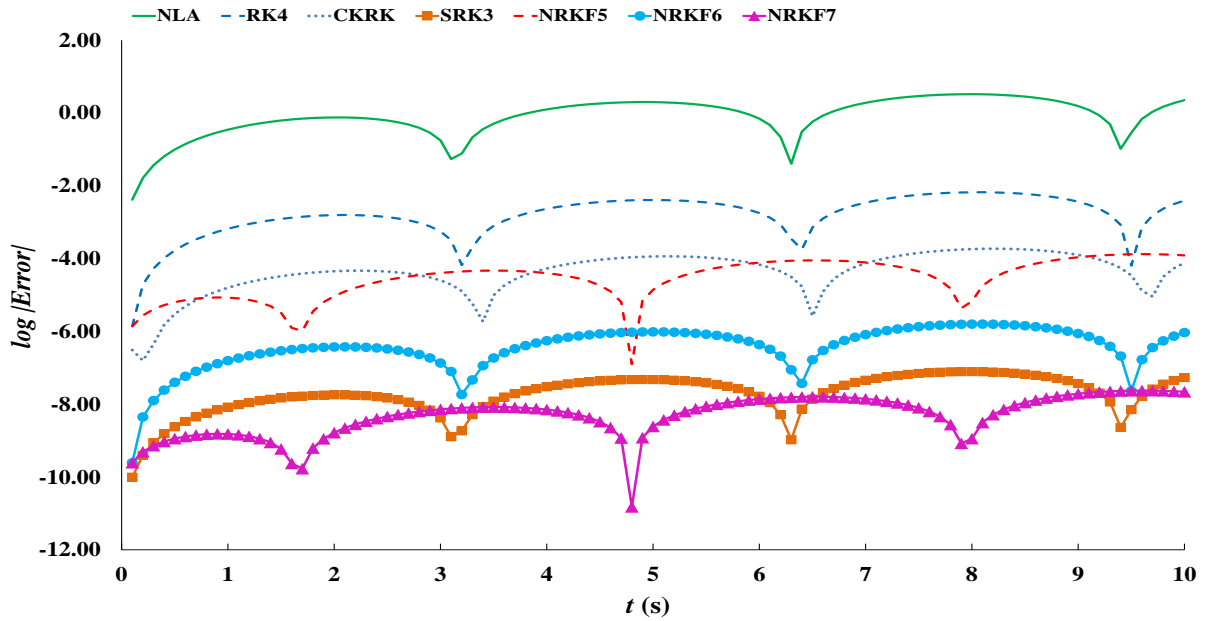


Fig. 8. Logarithmic error for different methods

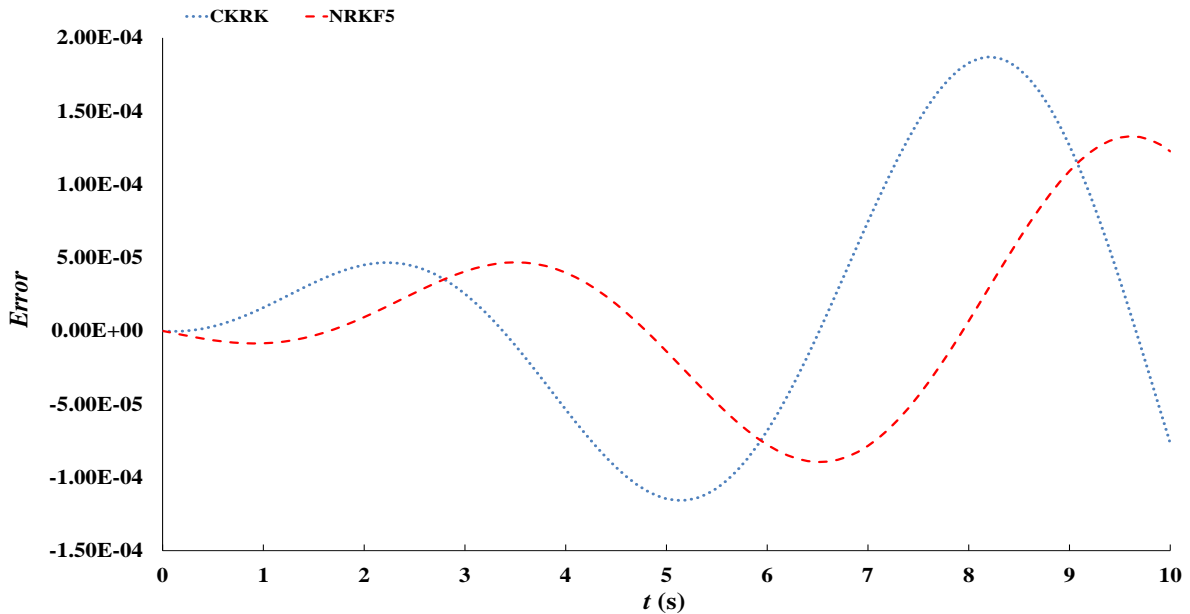


Fig. 9. Error comparison between the CKRK and NRKF5 schemes

According to Figure 8, the maximum values of the errors for the NRKF7 and SRK3 methods are equal to -7.625 and -7.105, respectively. Aside from this, as shown in Figure 9, the maximum values of errors are  $1.328 \times 10^{-3}$  and  $1.870 \times 10^{-3}$  for the NRKF5 and CKRK methods, respectively. In these comparisons, the NRKF5 and NRKF7 are explicit methods, although the CKRK and SRK3 methods are implicit schemes. The comparison between the maximum values of errors in these techniques illustrates that the proposed

explicit family has higher abilities in solving undamped systems, compared to the implicit methods.

### 7.2. Five Stories Shear Building with Non-Classical Damping

Figure 10 depicts a shear frame building, which was investigated by Rezaiee-Pajand et al. (2018). All stories have an equal mass of  $2.616 \times 10^6$  Kg. The stiffness of the second to fifth stories is considered as  $981 \times 10^6$  N/m. The stiffness of the first story is 20% larger than that of the other stories.

It should be added that the first story is equipped with a damping device. In this regard, the damping matrix consists of two parts. The classic damping of the structure is obtained by  $\mathbf{C}_c = 0.3\mathbf{M} + 0.002\mathbf{K}$ . Aside from this, the term  $20\mathbf{C}_c(1,1)$  is added to the damping of the first degree of freedom of the structure. As it is shown in Figure 10, five lateral forces are applied to the structure. The equation of these forces is given by:

$$\mathbf{f}(t) = 2.616 \times 10^6 \{1, 1, 1, 1, 1\}^T \sin(\pi t) \quad (42)$$

Selecting the time step as  $\Delta t = 0.01$  s, this example is analyzed using different techniques. The near-exact solution for this problem is obtained by the RK4 method with a very tiny time step equal to 0.00001 s. Figure 11 depicts the error of different methods in calculating the horizontal displacement of the fifth story compared to the near-exact solution.

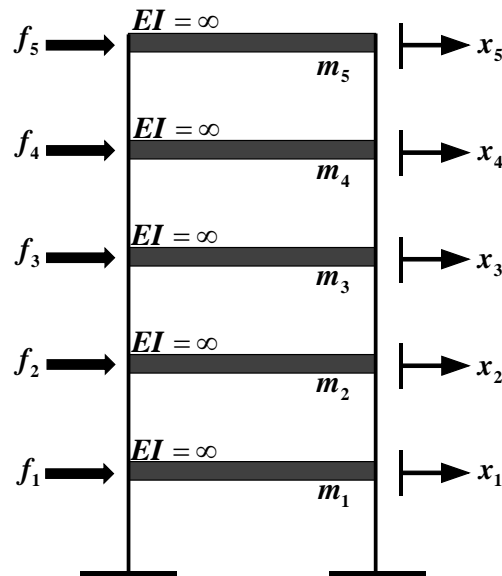


Fig. 10. Five stories shear building

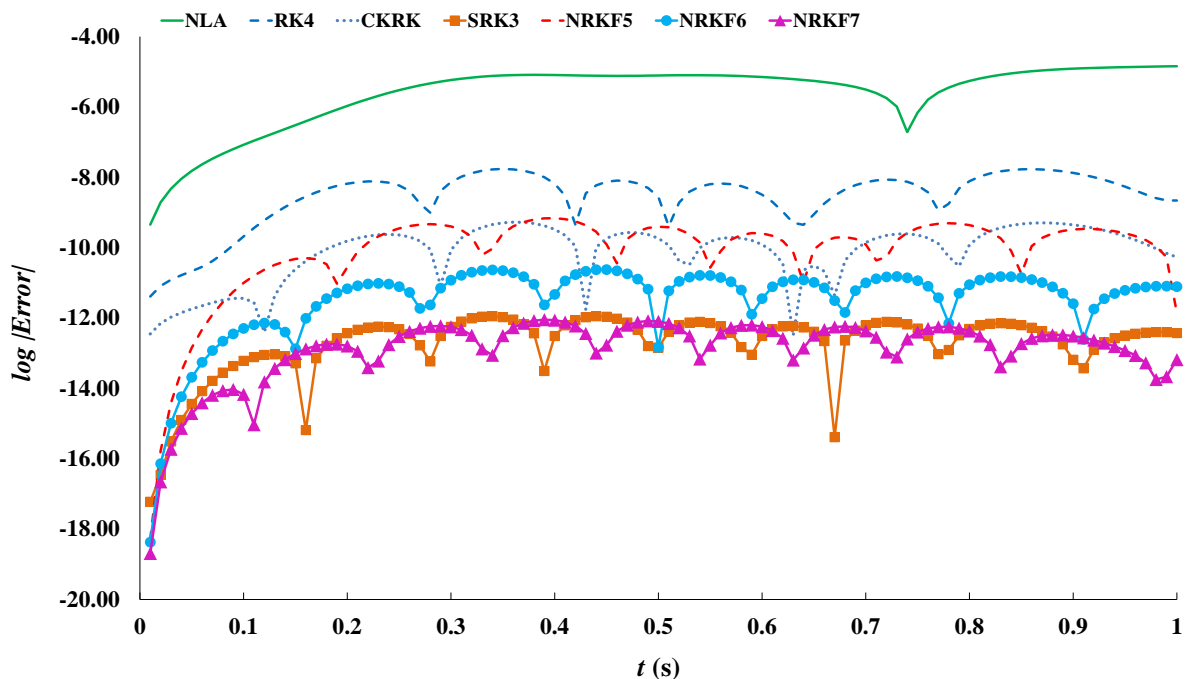


Fig. 11. Error of the horizontal displacement of the fifth story

Based on the results shown in Figure 11, the NRKF5 and CKRK methods have lower analysis errors compared to the NLA and RK4 schemes, which are more applicable time integration methods in civil engineering fields. The solution obtained by the NRKF6 is more accurate than the one from the implicit CKRK method. The 7<sup>th</sup>-order method of the new family and SRK3 technique furnished the best accuracy in the analysis. Figure 12 presents a more exact comparison between the error values of the NRKF7 and SRK3 methods. As it is illustrated in Figure 12, the value of error is larger in the SRK3 scheme compared to the NRKF7 method. The outcomes reveal that the accuracy of the proposed family in analyzing non-classic structural problems is better than the other methods.

### 7.3. A Structure with Two Degrees of Freedom Subjected to Impact Loading

Some researchers investigated a dynamic system with two degrees of freedom subjected to impact loading (Rezaiee-Pajand et al., 2018). The equilibrium equation of this system and the applied loads are expressed as follows.

$$\begin{bmatrix} m & 0 \\ 0 & 3m \end{bmatrix} \ddot{\mathbf{u}} + \begin{bmatrix} 3k & -2k \\ -2k & 6k \end{bmatrix} \mathbf{u} = \begin{bmatrix} 0 \\ 1 \end{bmatrix} \times f(t) \quad (43)$$

$$f(t) = \begin{cases} 1000(1-10t) & 0 \leq t \leq 0.1 \\ 0 & t \geq 0.1 \end{cases} \quad (44)$$

The values of stiffness  $k$  and mass  $m$  are equal to 1000 N/m and 0.5 Kg, respectively. The exact solution can be attained via modal analysis. By choosing a value of 0.001 s for the time step, the system is analyzed with different methods. The values of error for the time integration methods are shown in Figure 13. Based on the results obtained, the NLA method and the fourth-order classic Runge-Kutta lead to the highest errors in the analysis. The highest values of error for these methods are equal to -2.568 and -5.517, respectively. As it is demonstrated in the figure, the error of the analysis for the new family method decreases as the order of family increases. The highest values of error for the orders of 5, 6, and 7 are equal to -7.377, -9.309, and -11.290, respectively. Moreover, the NRKF7 method has better accuracy in comparison to the implicit SRK3 scheme. The results indicate that the proposed family is capable of analyzing structures subjected to impact loading over other techniques.

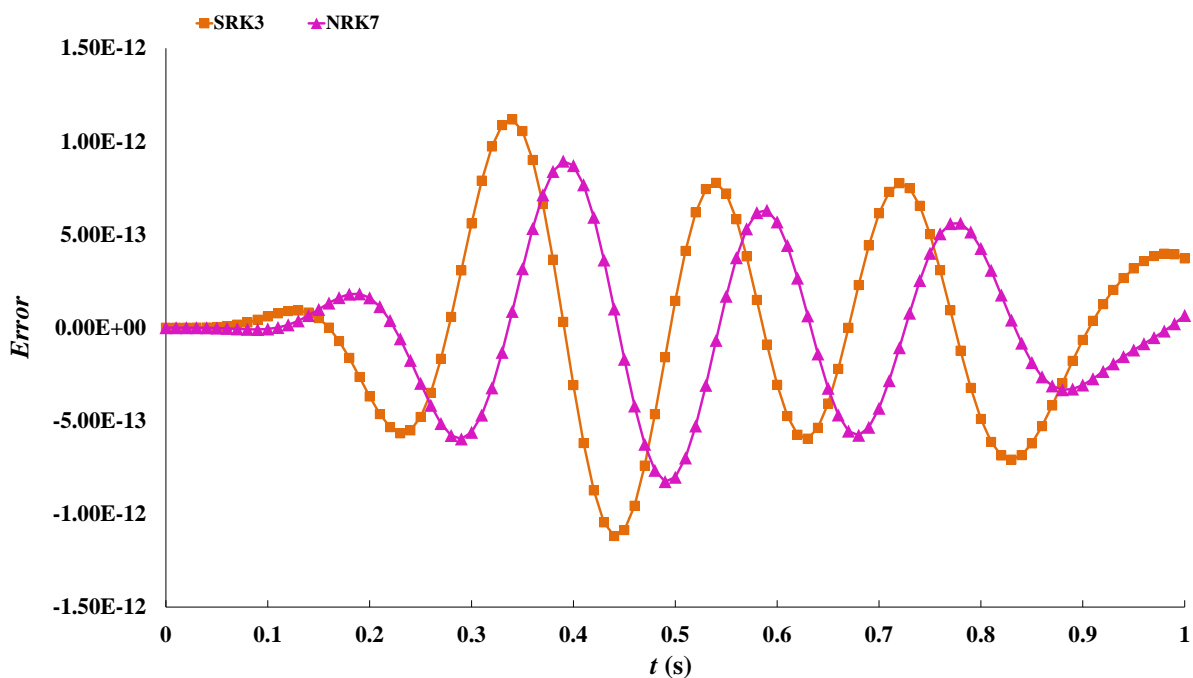


Fig. 12. Error comparison between the SRK3 and NRKF7 methods

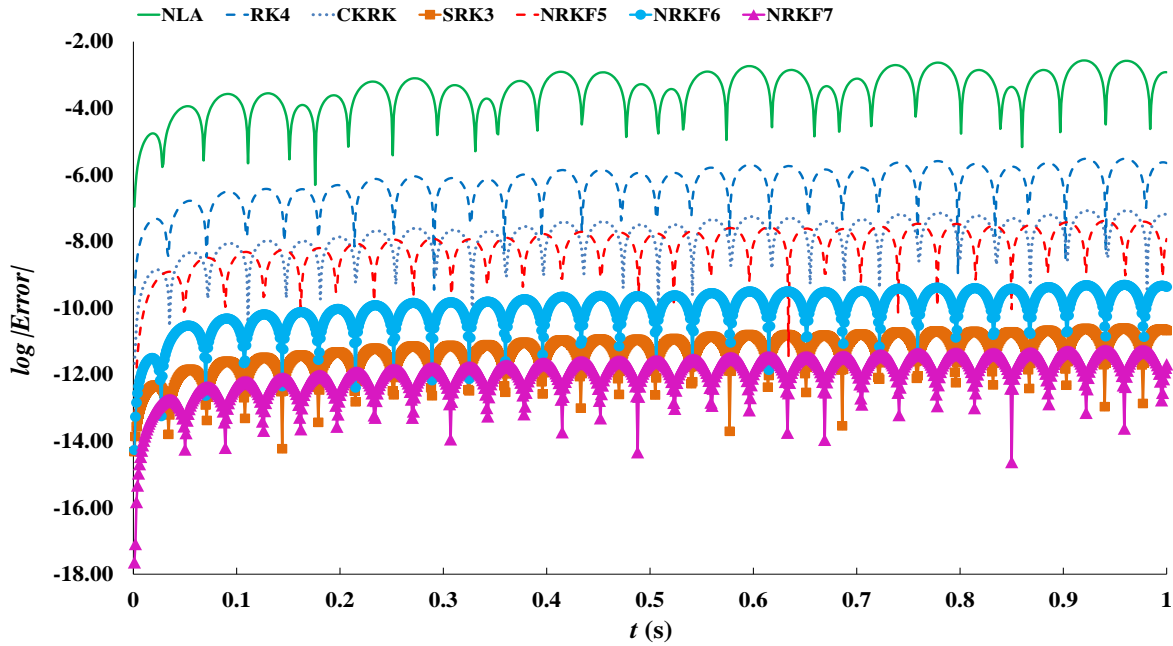


Fig. 13. Error of  $u_1$  of 2Dof structure

#### 7.4. Plane Truss

The plane truss represented in Figure 14 comprises three elements and 3 degrees of freedom (Paz and Kim, 2018). The characteristics of the members are outlined in Table 2. A constant horizontal force equal to 22241.108 N is applied to node 1. Figure 15 portrays the error value for horizontal displacement of this node in the final steps of the analysis. The related exact responses are obtained by using modal analysis.

The NRKF7 and NLA methods lead to the smallest and largest error values in the

analysis, respectively. The maximum values of the error for these methods are equal to -11.030 and -3.539, respectively. The error values of NRKF5 and CKRK schemes are nearly equal. The maximum value of error for these methods is almost equal to -7.588. Based on the results, it is obvious that an increase in the order of the new family reduces the error of the analysis. The results of this example demonstrated in Figure 15 illustrate that the suggested family is capable of analyzing two-dimensional structures.

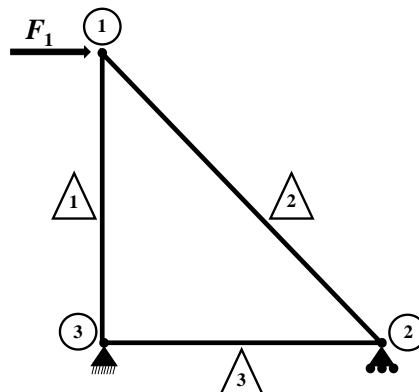


Fig. 14. Three members plane truss

Table 2. Characteristics of the plane truss

Member	Area (mm <sup>2</sup> )	Length (mm)	E (N/m <sup>2</sup> )	$\bar{m}$ (N.sec <sup>2</sup> /m <sup>2</sup> )
1	6451.6	1524.0	$2.06844 \times 10^{11}$	689.48
2	6451.6	2155.3	$2.06844 \times 10^{11}$	689.48
3	6451.6	1524.0	$2.06844 \times 10^{11}$	689.48

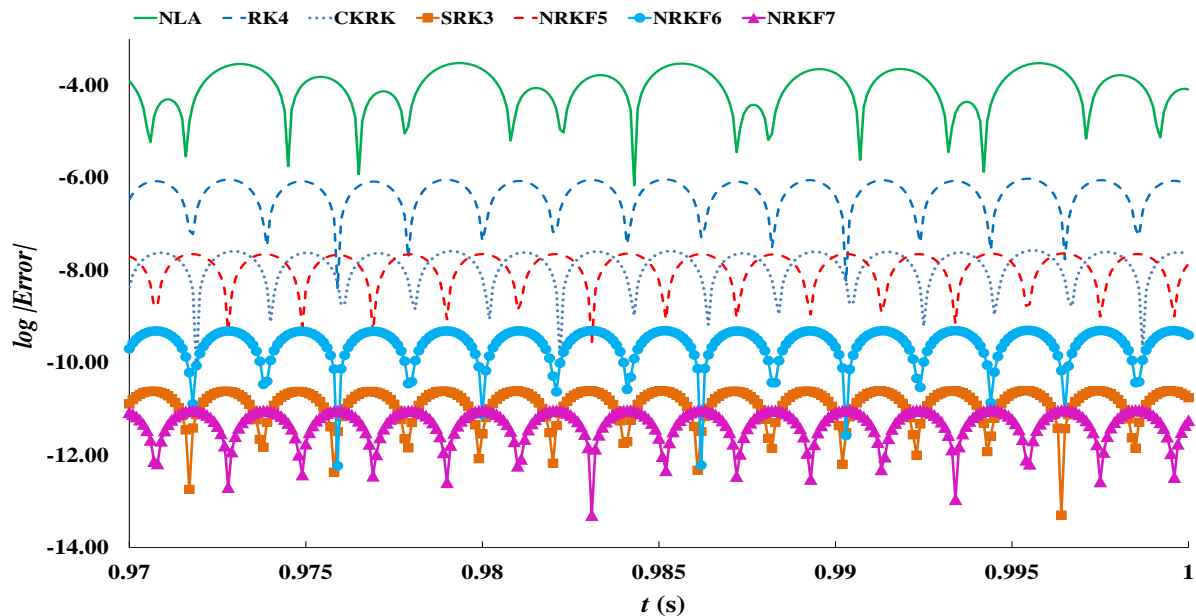


Fig. 15. The horizontal displacement error of node 1

### 7.5. Three-Dimensional Truss

The structure shown in Figure 16 illustrates a three-dimensional truss. The nodal coordinates are available in Table 3. The elastic modulus and density of members are given as  $E = 2 \times 10^{11}$  N/m<sup>2</sup> and  $\rho = 7850$  Kg/m<sup>3</sup>, respectively. In this structure, the upper node is subjected to two forces in the X- and Y-directions. These forces are equal to  $F_x = 4000$  kN and  $F_y = 16000$  kN. The cross-sectional area of highlighted members indicated by  $b$  is equal to 1935 mm<sup>2</sup>, and that of pale members

named  $a$  is equal to 3870 mm<sup>2</sup>. The smallest period of this structure is  $T_{min} = 2.59 \times 10^{-3}$  s. The responses of this structure are obtained up to  $t = 1.25 \times 10^6 T_{min}$  s by choosing the time steps of  $\Delta t = 0.01 T_{min}$  s. Figure 17 demonstrates the values of error in vertical tip displacement within the timeline  $[1247.5 \times 10^3 - 1250 \times 10^3] T_{min}$  s of the analysis. Moreover, the exact solution of the three-dimensional truss is available by using modal analysis.

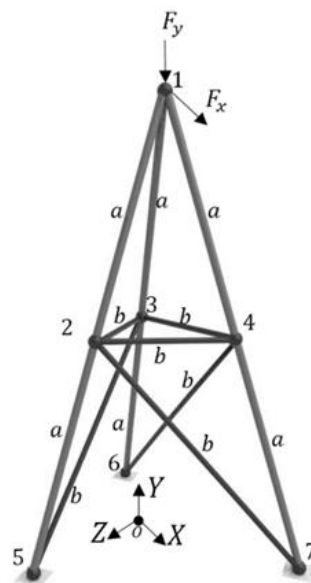
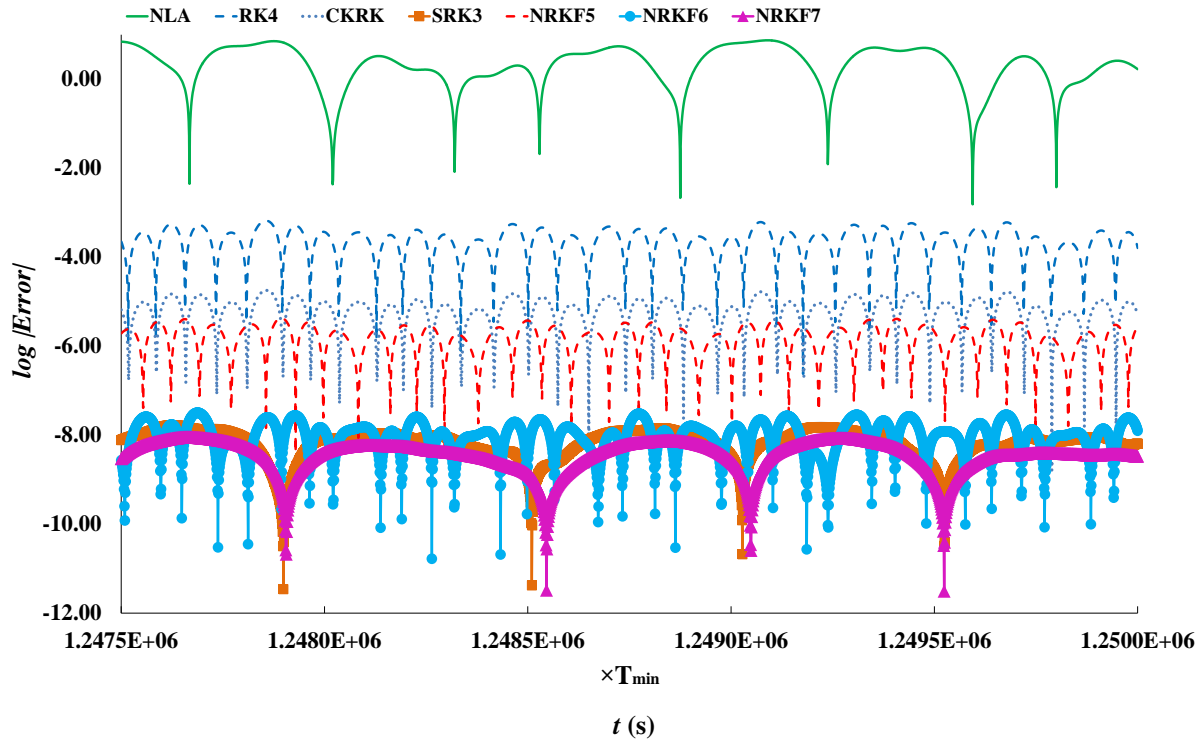


Fig. 16. The three-dimensional truss

**Table 3.** Characteristics of the three-dimensional truss

Node number	X (mm)	Y (mm)	Z (mm)
1	0	9144	0
2	0	4572	1524
3	-1219.2	4572	-914.4
4	1219.2	4572	-914.4
5	0	0	3048
6	-2438.4	0	-1828.8
7	2438.4	0	-1828.8

**Fig. 17.** Error of the top node vertical displacement

Error in each numerical integration method is calculated through Eq. (45).

$$Err = \sqrt{L_2 norm(x_{exact}(t) - x_{scheme}(t))} \quad (45)$$

$$L_2 norm(x(t)) = \sum_t (x(t))^2$$

Values of  $Err$  for different time integration methods and CPU time of each method are reported in Table 4.

The results presented in Figure 17 and Table 4 indicate that the highest accuracy belongs to the 7<sup>th</sup>-order method of the new family, while the Newmark linear acceleration technique leads to the lowest precision. The values of  $Err$  for these schemes are equal to  $2.69 \times 10^{-6}$  and  $2.34 \times 10^3$ , respectively. Based on the results obtained in Table 4, the fourth-order

Runge-Kutta method has the highest value in CPU time, which is equal to 146.11 s. On the other hand, the lowest value for CPU time with good accuracy is for the method NRKF5, which is equal to 69.53s. The NRKF7 method has a better performance compared to the SRK3 method in accuracy and CUP time. The values of  $Err$  and CPU time for the NRKF7 method are  $2.69 \times 10^{-6}$  and 84.84 s, and are  $4.87 \times 10^{-6}$  and 95.05 s for the SRK3 method. From the obtained results, one can conclude that the new explicit family has a good ability to analyze structural dynamic systems in low CPU time with acceptable accuracy. Furthermore, according to the outcomes, the present family methods show their ability in the analysis of three-dimensional problems.

### 7.6. A Nonlinear Mass-Spring-Damper System with 100 Dofs

Figure 18 illustrates a nonlinear system of masses, springs, and dampers with 100 Dofs. The relations for the forces applied due to nonlinear springs ( $F_{k,i}(x)$ ) and nonlinear dampers ( $F_{c,i}(\dot{x})$ ) are shown in Figure 19 (Rezaiee-Pajand and Karimi-Rad, 2017; Rezaiee-Pajand et al., 2021). The values for the masses ( $M_i$ ), and the coefficients  $K_i$  and  $C_i$ , are given in Table 5. The coefficients  $\beta_k$  and  $\beta_c$  are equal to 0.8. Also, for each nonlinear stiffness and damper, the values of  $u_x$  and  $v_x$  are equal to 1 m and 1 m/s, respectively.

No load is applied to the structure, and the initial displacement and velocity for all nodes are 0, except for the last node. The initial values for displacement and velocity of this node ( $x_{100}$  and  $\dot{x}_{100}$ ) are 2 m and 2 m/s, respectively. The near-exact solution is achieved by the fourth-order Runge-Kutta with a very tiny time step  $\Delta t_{ex} = \frac{\pi}{1.6\sqrt{3}} \times 10^{-3}$  s. Table 6 shows the results obtained by the various orders of the suggested family in the time interval of  $\left[0 - \frac{100\pi}{1.6\sqrt{3}}\right]$  s. Due to the explicitly of the fourth-order Runge-Kutta method, as well as, the new family, there is

no need for any iterative nonlinearity solution methods, such as Newton-Raphson iterations. The responses are obtained for three cases with different time steps ( $\Delta t$ ). The value of  $RMSE$ , the root of mean squares of the errors for all Dofs, can be obtained by the following equation.

$$RMSE_{scheme} = \sqrt{\frac{1}{steps} \times \sum_{i=1}^{100} \sum_{j=1}^{steps} (\mathbf{x}_{i,exact}(t_j) - \mathbf{x}_{i,scheme}(t_j))^2} \quad (46)$$

The results presented in Table 6 show that different orders of the new family can analyze properly nonlinear dynamic systems with many degrees of freedom. According to these results, as the order of the family increases, the value of  $RMSE$  decreases. Based on the experiments in Case 1 ( $\Delta t = 1000\Delta t_{ex}$ ), by increasing the order of the family, the solution becomes more stable. As shown by the numerical results, the NRKF5 method becomes unstable; however, the NRKF6 and NRKF7 schemes have more stable results. The results for Cases 2 and 3 reveal that for nonlinear dynamic analysis, the NRKF6 method can obtain solutions with low error, and even is more accurate than the NRKF7 method (Case 3). In this manner, the NRKF6 can be chosen as the optimum member of the new family, for nonlinear dynamic analysis.

**Table 4.** CPU time and error of various schemes

Scheme	NLA	RK4	CKRK	SRK3	NRKF5	NRKF6	NRKF7
CPU Time (s)	21.35	146.11	81.47	95.05	69.53	74.18	84.84
Err (mm)	$2.34 \times 10^3$	$2.01 \times 10^{-1}$	$5.44 \times 10^{-3}$	$4.87 \times 10^{-6}$	$1.37 \times 10^{-3}$	$8.88 \times 10^{-6}$	$2.69 \times 10^{-6}$

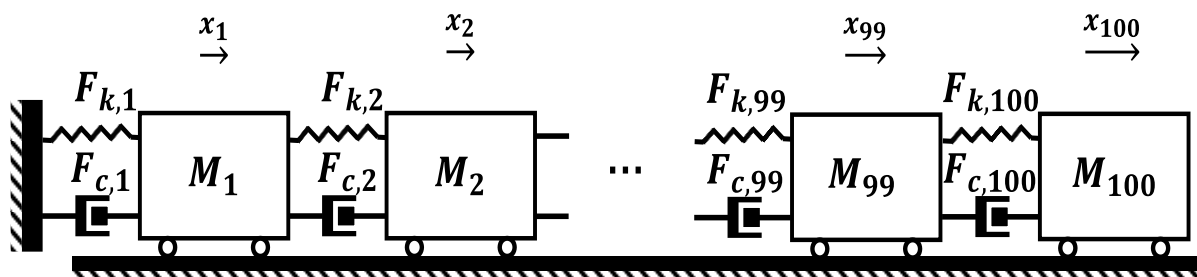


**Fig. 18.** The nonlinear mass-spring-damper system with 100 Dofs

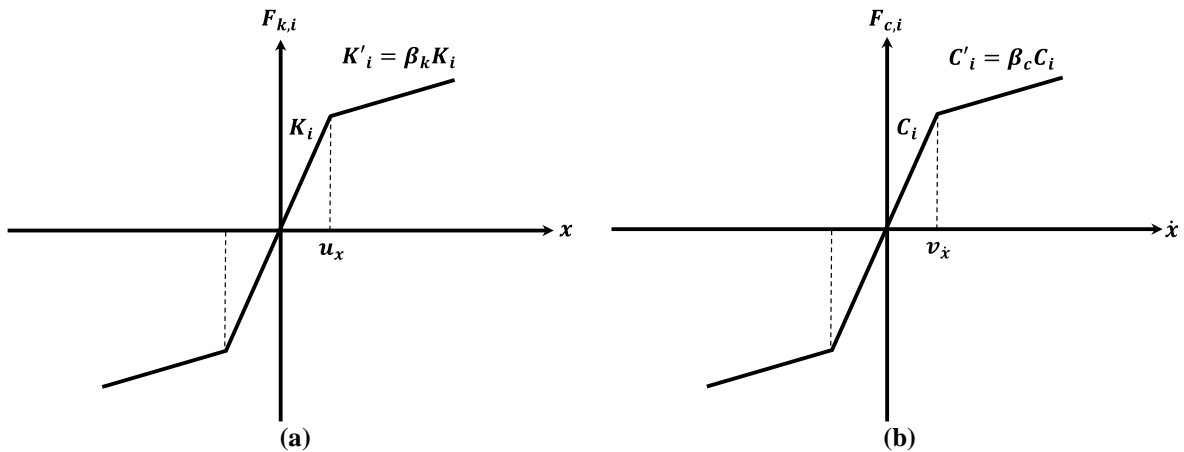


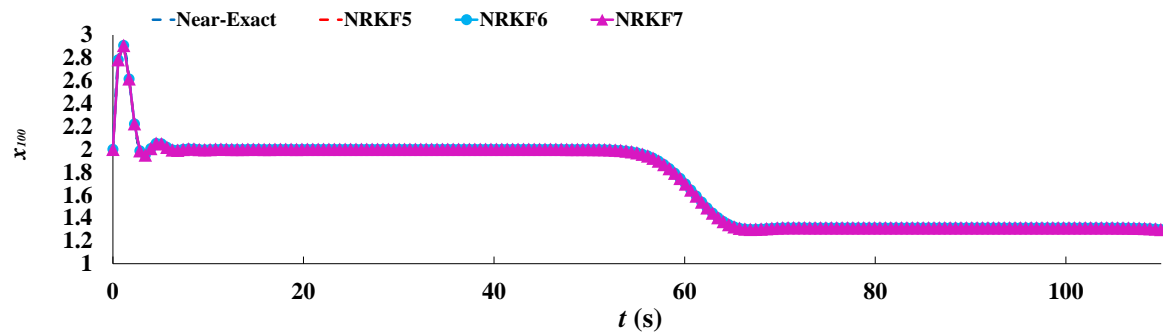
Fig. 19. Relations for stiffness and damping forces: a) Stiffness force; and b) Damping force

Table 5. The values of  $M_i$ ,  $K_i$  and  $C_i$  for various nodes

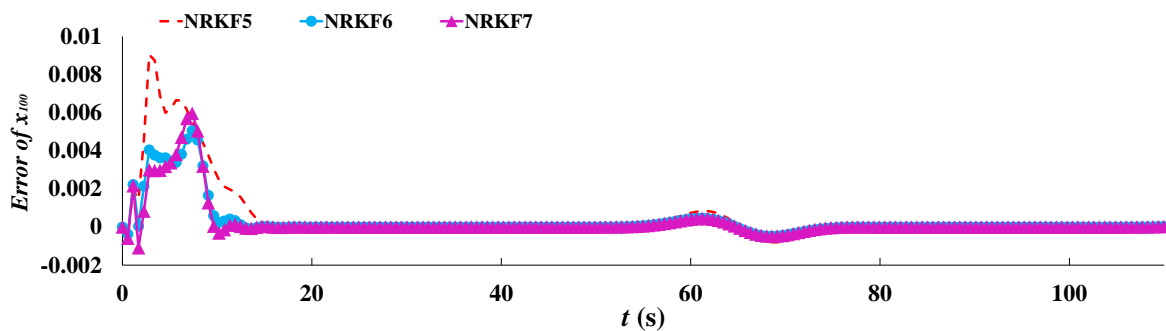
Number	$M_i$ (kg)	$K_i$ (N/m)	$C_i$ (N.s/m)
1-30	1	3	0.50
31-70	1	2	0.10
71-100	1	1	0.15

Table 6. The values of  $RMSE$  for the suggested family

Case.	$\Delta t$	Steps	RMSE		
			NRKF5	NRKF6	NRKF7
1	$1000\Delta t_{ex}$	100	$\infty$	$4.194 \times 10^1$	$3.521 \times 10^{-2}$
2	$500\Delta t_{ex}$	200	$6.222 \times 10^{-3}$	$3.569 \times 10^{-3}$	$3.493 \times 10^{-3}$
3	$100\Delta t_{ex}$	1000	$3.809 \times 10^{-4}$	$2.910 \times 10^{-4}$	$2.926 \times 10^{-4}$



(a)



(b)

Fig. 20. Solutions of  $x_{100}$  from various orders of the new family: a) The values of  $x_{100}$ ; and b) The errors of the solutions

Further to this, Figure 20 shows solutions of  $x_{100}$  by various orders of the new family obtained in the condition of Case 2. As shown in Figure 20, all orders of the new family have a good performance in achieving accurate results for nonlinear systems with many degrees of freedom. It is noteworthy that the smallest period of this structure is equal to 2.565 s and the time step chosen to analyze the system as shown in Case 2, is equal to 0.567 s ( $500 \Delta t_{ex}$ ), which means the time step used is not a very small value. Therefore, one can conclude that various orders of the new family have the capability in solving nonlinear systems with many degrees of freedom, in the case of using a logical time step.

### 7.7. A Tall Shear Building Subjected to El-Centro Ground Motion

In this example, the dynamics of a tall

shear building subjected to a realistic ground motion are analyzed. This shear building shown in Figure 21 is a fifty-story structure. The nonlinear behavior of the structure has been assumed as the bilinear model demonstrated in Figure 22. The elastic stiffness is  $K_1 = 3.404 \times 10^5$  N/m and the post-elastic stiffness is  $K_2 = 3.404 \times 10^4$  N/m.  $u_x$  is considered as 0.012 m. The story mass is  $m = 245.6 \times 10^3$  Kg. The mentioned characteristics are the same for all stories.

Since the dynamic response of structures due to earthquake excitations is very important in earthquake engineering, the fifty-story shear building is analyzed when it is subjected to the El-Centro earthquake. Figure 23 shows the time history of the North-South component of this ground motion.

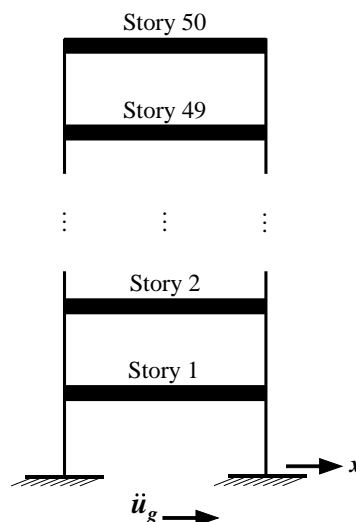


Fig. 21. A tall shear building with fifty stories

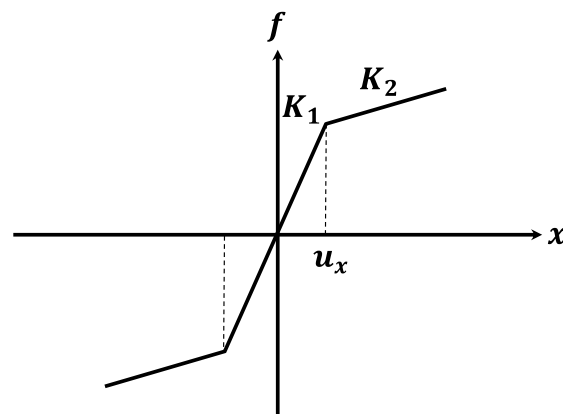


Fig. 22. Nonlinear relation between deformation and force

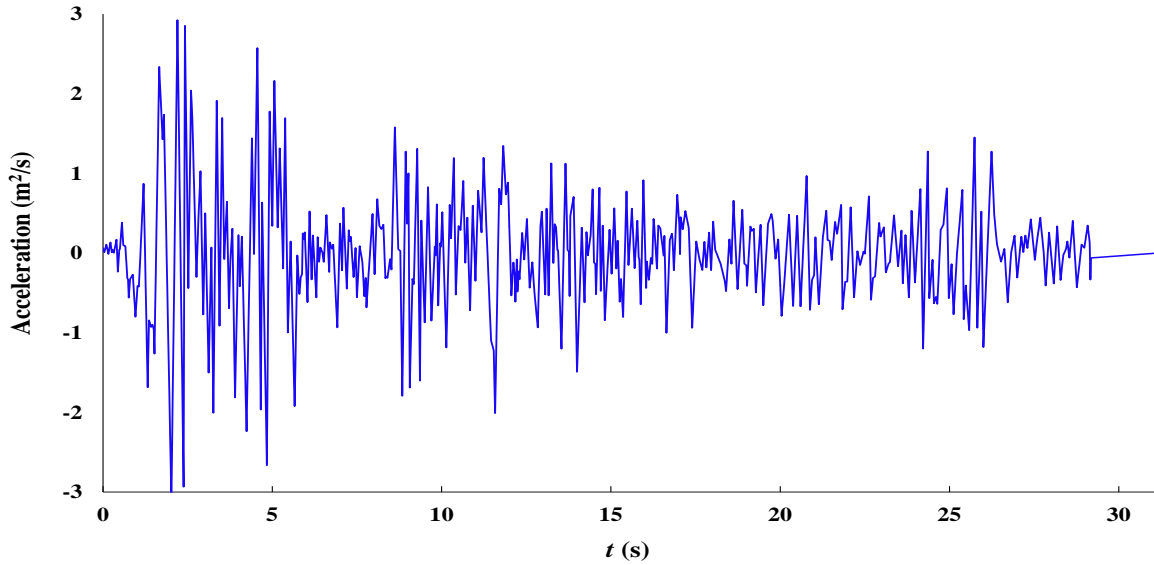


Fig. 23. Time history of north-south component of the El-Centro ground motion

The near-exact solution of this analysis is obtained by the fourth-order Runge-Kutta method using a very tiny time step  $\Delta t_{ex} = 2 \times 10^{-5}$  s in the time interval of 31.18 s. To investigate the advantages of the new methods, the structure is analyzed with various time steps  $\Delta t_1 = 2000\Delta t_{ex}$ ,  $\Delta t_2 = 1000\Delta t_{ex}$  and  $\Delta t_3 = 100\Delta t_{ex}$ . Also, the results are compared to those from the generalized- $\alpha$  and SRK3 methods. Due to the explicitness of the new family, there is no

need for iterative methods such as Newton-Raphson technique. However, the generalized- $\alpha$  and SRK3 schemes need Newton-Raphson iterations. The iterations are terminated if the incremental displacements reach a tiny value,  $10^{-10}$  m. Figure 24 shows the lateral responses of the first story analyzed by various methods, which are obtained by using the second time step,  $\Delta t_2$ .

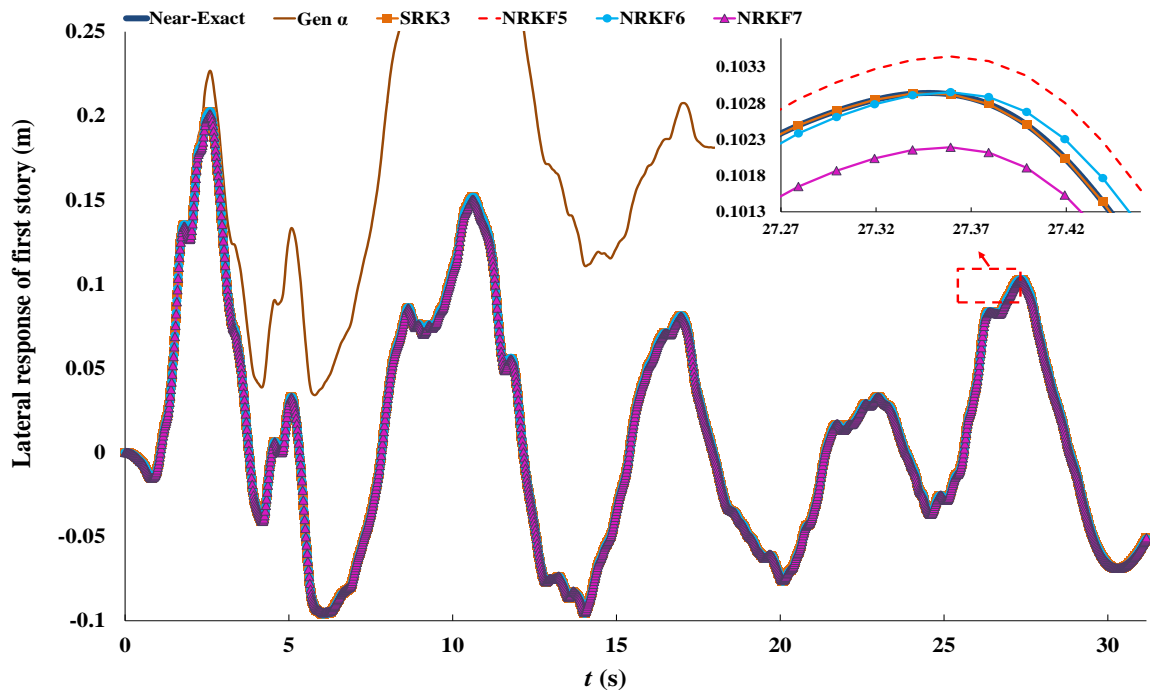


Fig. 24. lateral responses of the first story analyzed by various methods with the second time step,  $\Delta t_2$

**Table 7.** Values of analysis error, CPU time, and storage for different methods

Scenario	Property	Gen. $\alpha$	NRKF5	NRKF6	NRKF7	SRK3
$\Delta t_1$	<i>Err</i>	$1.90 \times 10^1$	1.22	1.22	1.21	$1.71 \times 10^{-1}$
	CPU Time (s)	1127	38	43	51	384
	Storage (Byte)	1,002,912	726,824	729,680	732,664	742,177
$\Delta t_2$	<i>Err</i>	8.26	$6.51 \times 10^{-3}$	$5.72 \times 10^{-3}$	$7.06 \times 10^{-3}$	$2.68 \times 10^{-6}$
	CPU Time (s)	2540	71	86	98	582
	Storage (Byte)	1,938,912	1,350,024	1,352,880	1,355,864	1,365,377
$\Delta t_3$	<i>Err</i>	$2.63 \times 10^{-1}$	$6.56 \times 10^{-4}$	$5.75 \times 10^{-4}$	$7.13 \times 10^{-4}$	$5.85 \times 10^{-8}$
	CPU Time (s)	21980	676	821	961	4279
	Storage (Byte)	18,776,112	12,574,824	12,577,680	12,580,664	12,590,177

In order to compare analysis error (*Err*), CPU time, and storage values achieved by various time integration methods, Table 7 is prepared. In this table, the value of analysis error (*Err*) is calculated by using Eq. (45). Based on the results presented in Table 7, the generalized- $\alpha$  method with the highest values in *Err*, CPU time, and storage, has the weakest performance among the other methods. On the other hand, the NRKF5 method reaches the minimum values in CPU time and storage, in various analyzes. In the second and third scenarios (the cases of  $\Delta t_2$  and  $\Delta t_3$ ), among different orders of the new family, the NRKF6 method reaches solutions with the minimum values in *Err* and comparable values in CPU time and storage. Therefore, the NRKF6 method is chosen as the best order among different orders of the new family, which can reach better solutions in the nonlinear dynamic analysis. Compared to the SRK3 method, all suggested members of the new family have lower values in CPU time and storage. The values of *Err* obtained for the SRK3 method are small in different scenarios, whereas, compared to different members of the new family, the SRK3 method has larger values in CPU time.

By comparing the results obtained by the SRK3 method in the first scenario ( $\Delta t_1$ ) and those by the NRKF6 method in the second scenario ( $\Delta t_2$ ), it is obvious that the NRKF6 method has a better performance to obtain solutions with lower error values in a lower CPU time. In this comparison, the values of *Err* for the SRK3 and NRKF6 methods are  $1.71 \times 10^{-1}$  and  $5.72 \times 10^{-3}$ , respectively. Also, the values of CPU time for these

methods are 384 s and 86 s, respectively. Aside from this, by comparing the values of CPU time between these two methods, one can see that the ratio of the CPU time values of the SRK3 and NRKF6 methods is  $8.9 \left( \frac{384}{43} \right)$  in the first scenario. The ratio is equal to  $6.8 \left( \frac{582}{86} \right)$  and  $5.2 \left( \frac{4279}{821} \right)$  in the second and third scenarios, respectively. These comparisons illustrate that the SRK3 method needs a higher interval of time to perform nonlinear dynamic analyses compared to the NRKF6 method. On the other hand, the NRKF6 method can obtain good solutions with low error values in a shorter CPU time.

## 8. Conclusions

In this study, a higher-order explicit family of time integration methods was presented. The suggested formulation could analyze various linear and nonlinear dynamic systems. To develop this family, the Taylor series of the analytical amplification matrix was utilized. In this way, each time step of the integration procedure was divided into several stages. Different orders of the suggested family can be obtained by solving a system of nonlinear algebraic equations. The coefficients required ( $\alpha$ ) were shown for the orders  $n = 2$  to 10, in Table 1. It is worth mentioning that the higher-order methods can be achieved effortlessly. Therefore, the proposed methods form a comprehensive family. As a negative point, the stability of the proposed family is conditional. On the other

hand, as a positive point, the numerical accuracy and order of accuracy are improved as the order of the family increases.

One of the superiorities of the proposed Runge-Kutta family is the equality between the order of accuracy of the family and its number of stages used in a single time step. The results showed that the new family had the desired amplitude decay with a better performance in period error value compared to two well-known numerical integration methods, the Newmark linear acceleration and fourth-order Runge-Kutta. Furthermore, the performance of the family in amplitude decay and period error was enhanced as the order ( $n$ ) rises.

The advantages of the authors' schemes were illustrated through various numerical experiments over several useful time integration methods, such as the Newmark linear acceleration technique, generalized- $\alpha$ , and explicit and implicit Runge-Kutta methods. The example undamped single degree of freedom oscillator showed the superiority of the proposed methods over the other techniques in analyzing linear mechanical systems. Furthermore, the results obtained by the proposed explicit family were more accurate than those achieved by the implicit CKRK and SRK3 methods. In Example 7-3, an impact load was applied to two degrees of freedom structure. The results demonstrated that the NRKF7 method has a better performance in analyzing a structure subjected to impact loading compared to the implicit SRK3 method. The methods NRKF6 and NRKF5 had more accurate results than the CKRK, fourth-order Runge-Kutta, and Newmark linear acceleration methods. The outcomes from Example 7-2 illustrated the ability of the new family in dealing with the non-classical damping behavior resulting from a five-story shear building. This example demonstrated that the method NRKF7 was the most accurate technique in analyzing shear building structures with non-classical dampers. Examples 7-4 and 7-5 showed that the suggested methods can solve plane and

three-dimensional truss problems with high accuracy. In Example 7-5, the method NRKF6 and NRKF7 had the highest performance to solve the 3D truss problem in a low CPU time with very good accuracy. The results illustrated that Newmark linear acceleration and the fourth-order Runge-Kutta methods had the highest values in error and CPU time, respectively.

Example 7-6 showed that all orders of the proposed family can solve many degrees of freedom mass-spring-damper systems with nonlinear properties in stiffness and damping. In this experiment, the method NRKF7 analyzed the system with the lowest value in error, for large and medium time steps. However, if the time step is chosen a tiny value, the method NRKF6 can result in the more accurate analysis. As a weak point, if the time step is selected a large value, the results show that the lower orders of the family become unstable. However, as the order of the family is boosted, the stability, as well as, the accuracies of the answers are increased, which is a positive point.

In the last example, a tall shear building structure subjected to El-Centro ground motion was investigated. This structure had many degrees of freedom with nonlinear behavior in stiffness. According to the results, the existing implicit methods in this example, the generalized- $\alpha$  and SRK3 techniques had the highest values in error and CPU time, respectively. On the other hand, all members of the proposed family had the lowest values in CPU storage. As well, all orders of the proposed family had good performances in the accuracy of the solutions. Further to this, the NRKF6 method, which was chosen as the best order of the new family, could obtain accurate solutions with low values in CPU time and storage. This experiment illustrated that the new family methods are robust in analyzing tall building structures subjected to a realistic load, such as El-Centro ground motion.

## 9. Declarations

It is confirmed that the availability of data and material, funding, authors' contributions, acknowledgements, and all the subheadings of these and also the relevant information under each have been declared in this paper. Moreover, there is no conflict of interest.

## 10. References

- Bathe, K.J. (1982). *Finite Element procedures in engineering analysis*, Prentice Hall, United Kingdom.
- Bathe, K.J. and Wilson, E.L. (1972). "Stability and accuracy analysis of direct integration methods", *Earthquake Engineering and Structural Dynamics*, 1(3), 283-291, <https://doi.org/10.1002/eqe.4290010308>.
- Braś, M., Izzo, G. and Jackiewicz, Z. (2017). "Accurate implicit-explicit general linear methods with inherent Runge-Kutta stability", *Journal of Scientific Computing*, 70(3), 1105-1143, <https://doi.org/10.1007/s10915-016-0273-y>.
- Brogan, W.L. (1991). *Modern control theory*, Prentice Hall, United Kingdom.
- Butcher, J.C. (2016). *Numerical methods for ordinary differential equations*, Wiley, Germany.
- Chang, S.Y. (2013). "An explicit structure-dependent algorithm for pseudodynamic testing", *Engineering structures*, 46, 511-525, <https://doi.org/10.1016/j.engstruct.2012.08.009>.
- Chung, J. and Hulbert, G. (1993). "A time integration algorithm for structural dynamics with improved numerical dissipation: the generalized- $\alpha$  method", *Journal of Applied Mechanics*, 60(2), 371-375, <https://doi.org/10.1115/1.2900803>.
- Ezoddin, A., Kheyroddin, A. and Gholhaki, M. (2020). "Investigation of the effects of link beam length on the RC frame retrofitted with the linked column frame system", *Civil Engineering Infrastructures Journal*, 53(1), 137-159, <https://doi.org/10.22059/CEIJ.2019.280596.1580>.
- Fok, P.W. (2016). "A linearly fourth order multirate Runge-Kutta method with error control", *Journal of Scientific Computing*, 66(1), 177-195, <https://doi.org/10.1007/s10915-015-0017-4>.
- Ghassemieh, M. and Badrkhani Ajaei, B. (2018). "Impact of integration on straining modes and shear-locking for plane stress Finite Elements", *Civil Engineering Infrastructures Journal*, 51(2), 425-443, <https://doi.org/10.7508/CEIJ.2018.02.011>.
- Goel, M.D., Kumar, M. and Matsagar, V.A. (2018). "Blast mitigation analysis of semi-buried structure", *Civil Engineering Infrastructures Journal*, 51(2), 445-460, <https://doi.org/10.7508/CEIJ.2018.02.012>.
- Grote, M.J., Mehlin, M. and Mitkova, T. (2015). "Runge-Kutta-based explicit local time-stepping methods for wave propagation", *SIAM Journal on Scientific Computing*, 37(2), A747-A775, <https://doi.org/10.1137/140958293>.
- Gu, Y. and Zhu, Y. (2021). "Adams predictor-corrector method for solving uncertain differential equation", *Computational and Applied Mathematics*, 40(2), 1-20, <https://doi.org/10.1007/s40314-021-01461-2>.
- Hairer, E., Lubich, C. and Wanner, G. (2006). *Geometric numerical integration: Structure-preserving algorithms for ordinary differential equations*, Springer Berlin, Heidelberg.
- Heun, K. (1900). "Neue Methoden zur approximativen integration der differentialgleichungen einer unabhängigen veränderlichen", *Zeitschrift für Angewandte Mathematik und Physik*, 45, 23-38.
- Hughes, T.J. (2012). *The Finite Element method: Linear static and dynamic Finite Element analysis*, Dover Publications, United States.
- Hulbert, G.M. and Chung, J. (1996). "Explicit time integration algorithms for structural dynamics with optimal numerical dissipation", *Computer Methods in Applied Mechanics and Engineering*, 137(2), 175-188, [https://doi.org/10.1016/S0045-7825\(96\)01036-5](https://doi.org/10.1016/S0045-7825(96)01036-5).
- Hulbert, G.M. and Hughes, T.J.R. (1987). "An error analysis of truncated starting conditions in step-by-step time integration: Consequences for structural dynamics", *Earthquake Engineering and Structural Dynamics*, 15(7), 901-910, <https://doi.org/10.1002/eqe.4290150710>.
- Isherwood, L., Grant, Z.J. and Gottlieb, S. (2018). "Strong stability preserving integrating factor Runge-Kutta methods", *SIAM Journal on Numerical Analysis*, 56(6), 3276-3307, <https://doi.org/10.1137/17M1143290>.
- Izzo, G. and Jackiewicz, Z. (2017). "Highly stable implicit-explicit Runge-Kutta methods", *Applied Numerical Mathematics*, 113(March), 71-92, <https://doi.org/10.1016/j.apnum.2016.10.018>.
- Jørgensen, J.B., Kristensen, M.R. and Thomsen, P.G. (2018). "A family of ESDIRK integration methods", *arXiv preprint arXiv:1803.01613*, <https://doi.org/10.48550/arXiv.1803.01613>.
- Kassam, A.K. and Trefethen, L.N. (2005). "Fourth-order time-stepping for stiff PDEs", *SIAM Journal on Scientific Computing*, 26(4), 1214-1233, <https://doi.org/10.1137/S1064827502410633>.
- Kim, W. (2019). "A new family of two-stage explicit

- time integration methods with dissipation control capability for structural dynamics”, *Engineering Structures*, 195(15 September), 358-372, <https://doi.org/10.1016/j.engstruct.2019.05.095>.
- Kordi, A. and Mahmoudi, M. (2022). “Damage detection in truss bridges under moving load using time history response and members influence line curves”, *Civil Engineering Infrastructures Journal*, 55(1), 183-194, <https://doi.org/10.22059/CEIJ.2021.314109.1723>.
- Kutta, W. (1901). “Beitrag zur näherungsweise Integration totaler Differentialgleichungen”, *Zeitschrift für Angewandte Mathematik und Physik*, 46, 435-453.
- Martín-Vaquero, J. and Kleefeld, A. (2019). “ESERK5: A fifth-order extrapolated stabilized explicit Runge-Kutta method”, *Journal of Computational and Applied Mathematics*, 356(15 August), 22-36, <https://doi.org/10.1016/j.cam.2019.01.040>.
- Lee, T.Y., Chung, K.J. and Chang, H. (2017). “A new implicit dynamic finite element analysis procedure with damping included”, *Engineering Structures*, 147(15 September), 530-544, <https://doi.org/10.1016/j.engstruct.2017.06.006>.
- Moler, C. and Van Loan, C. (2003). “Nineteen dubious ways to compute the exponential of a matrix, twenty-five years later”, *SIAM Review*, 45(1), 3-49, <https://doi.org/10.1137/S00361445024180>.
- Haj Najafi, L. and Tehranizadeh, M. (2016). “Distribution of building nonstructural components in height subjected to cost of damage for low-rise office buildings”, *Civil Engineering Infrastructures Journal*, 49(2), 173-196, <https://doi.org/10.7508/ceij.2016.02.001>.
- Newmark, N.M. (1959). “A method of computation for structural dynamics”, *Journal of the Engineering Mechanics Division*, 85(3), 67-94, <https://doi.org/10.1061/JMCEA3.0000098>.
- Noels, L., Stainier, L. and Ponthot, J.P. (2006). “Energy conserving balance of explicit time steps to combine implicit and explicit algorithms in structural dynamics”, *Computer Methods in Applied Mechanics and Engineering*, 195(19-22), 2169-2192, <https://doi.org/10.1016/j.cma.2005.03.003>.
- Ortigosa, R., Gil, A.J., Martínez-Frutos, J., Franke, M. and Bonet, J. (2020). “A new energy-momentum time integration scheme for nonlinear thermo-mechanics”, *Computer Methods in Applied Mechanics and Engineering*, 372(1 December), 113395, <https://doi.org/10.1016/j.cma.2020.113395>.
- Paz, M. and Kim, Y.H. (2018). *Structural Dynamics: Theory and Computation*, Springer International Publishing, Germany.
- Rezaiee, F., Fakhradini, S.M. and Ghahremannejad, M. (2018). “Numerical evaluation of progressive collapse potential in reinforced concrete buildings with various floor plans due to single column removal”, *Civil Engineering Infrastructures Journal*, 51(2), 405-424, <https://doi.org/10.7508/ceij.2018.02.010>.
- Rezaiee-Pajand, M., Esfehiani, S.A.H. and Karimi-Rad, M. (2018). “Highly accurate family of time integration method”, *Structural Engineering and Mechanics*, 67(6), 603-616, <https://doi.org/10.12989/sem.2018.67.6.603>.
- Rezaiee-Pajand, M., Esfehiani, S.A.H. and Ehsanmanesh, H. (2021). “An efficient weighted residual time integration family”, *International Journal of Structural Stability and Dynamics*, 21(08), 2150106, <https://doi.org/10.1142/S0219455421501066>.
- Rezaiee-Pajand, M. and Karimi-Rad, M. (2017). “An accurate predictor-corrector time integration method for structural dynamics”, *International Journal of Steel Structures*, 17(3), 1033-1047, <https://doi.org/10.1007/s13296-017-9014-9>.
- Rossi, D.F., Ferreira, W.G., Mansur, W.J. and Calenzani, A.F.G. (2014). “A review of automatic time-stepping strategies on numerical time integration for structural dynamics analysis”, *Engineering Structures*, 80, 118-136, <https://doi.org/10.1016/j.engstruct.2014.08.016>.
- Shutov, A.V., Landgraf, R. and Ihlemann, J. (2013). “An explicit solution for implicit time stepping in multiplicative finite strain viscoelasticity”, *Computer Methods in Applied Mechanics and Engineering*, 265(1 October), 213-225, <https://doi.org/10.1016/j.cma.2013.07.004>.
- Soares, D. (2016). “A novel family of explicit time marching techniques for structural dynamics and wave propagation models”, *Computer Methods in Applied Mechanics and Engineering*, 311(1 November), 838-855, <https://doi.org/10.1016/j.cma.2016.09.021>.
- Soares, D. and Großholz, G. (2018). “Nonlinear structural dynamic analysis by a stabilized central difference method”, *Engineering Structures*, 173, 383-392, <https://doi.org/10.1016/j.engstruct.2018.06.115>.
- Sun, Z. and Shu, C.W. (2019). “Strong stability of explicit Runge-Kutta time discretizations”, *SIAM Journal on Numerical Analysis*, 57(3), 1158-1182, <https://doi.org/10.1137/18M122892X>.
- Turaci, M.Ö. and Öziş, T. (2018). “On explicit two-derivative two-step Runge-Kutta methods”, *Computational and Applied Mathematics*, 37(5), 6920-6954, <https://doi.org/10.1137/18M122892X>.
- Turyn, L. (2013). *Advanced engineering mathematics*, CRC Press, United States.
- Veju, P., George, A. and Rahulkar, A.D. (2016). “Comparative study on the computation of state transition matrix using La-grange's interpolation

technique and Cayley-Hamilton theorem”, *Proceedings of the 10<sup>th</sup> International Conference on Intelligent Systems and Control (ISCO)*, Coimbatore, India, [10.1109/ISCO.2016.7726936](https://doi.org/10.1109/ISCO.2016.7726936).

Yaghoubi, V., Abrahamsson, T. and Johnson, E.A. (2016). “An efficient exponential predictor-corrector time integration method for structures with local nonlinearity”, *Engineering Structures*, 128, 344-361, <https://doi.org/10.1016/j.engstruct.2016.09.024>.

Zhang, L., Zhang, Q. and Sun, H.W. (2020). “Exponential Runge-Kutta method for two-dimensional nonlinear fractional complex Ginzburg-Landau equations”, *Journal of Scientific Computing*, 83(3), 1-24, <https://doi.org/10.1007/s10915-020-01240-x>.

Zhao, S. and Wei, G.W. (2014). “A unified discontinuous Galerkin framework for time integration”, *Mathematical Methods in the Applied Sciences*, 37(7), 1042-1071, <https://doi.org/10.1002/mma.2863>.



This article is an open-access article distributed under the terms and conditions of the Creative Commons Attribution (CC-BY) license.

## Appendices

### A.1. The Uniqueness of the Coefficients

$\alpha_j$

One can consider  $\mathbf{A}^n = \{\alpha_1^n, \alpha_2^n, \dots, \alpha_{n-1}^n\}$  as a set of the coefficients  $\alpha_j$  for  $j = 2, \dots, n-1$  calculated from the nonlinear algebraic system given in Eq. (18) with the order of  $n$ . For every set of  $\mathbf{A}^n$ , there is another set, such as  $\mathbf{B}^n = \{\beta_1^n, \beta_2^n, \dots, \beta_{n-1}^n\}$  with the following relationships, which is a dual solution for the nonlinear algebraic system.

$$\begin{aligned} \beta_1^n &= \alpha_{n-2}^n \\ \beta_2^n &= \alpha_{n-3}^n \\ &\dots \\ \beta_{n-2}^n &= \alpha_1^n \\ \beta_{n-1}^n &= \alpha_{n-1}^n \end{aligned} \tag{A1}$$

One can easily check the equality of these dual sets ( $\mathbf{A}^n$  and  $\mathbf{B}^n$ ) for Eq. (18). It is worth mentioning that numerical

characteristics of the new methods performed by the solutions  $\mathbf{A}^n$  and  $\mathbf{B}^n$ , such as stability, order of accuracy, and numerical accuracy, are similar. For the new methods with the values of  $n$  equal to 2, 3, and 4, the sets  $\mathbf{A}^n$  and  $\mathbf{B}^n$  are equal. Therefore, the coefficients for  $n = 2, 3$ , and 4, can be obtained uniquely.

### A.2. The Existence of the Coefficients $\alpha_j$

The coefficients  $\alpha_{n-1}^n$  and  $\alpha_{n-2}^n$  are obtained based on the second and last equations in Eq. (18). Form the equality  $\frac{n-1}{1 + \sum_{j=1}^{n-1} \frac{1}{\alpha_j}} = \frac{1}{2!}$ ,  $\alpha_{n-1}^n$  is calculated using the other coefficients as follows.

$$\alpha_{n-1}^n = \frac{1}{2n-3 - \sum_{j=1}^{n-2} \frac{1}{\alpha_j}} \tag{A2}$$

Also,  $\alpha_{n-2}^n$  can be obtained from the equalities  $\frac{\prod_{v=1}^{n-2} \alpha_v}{1 + \sum_{j=1}^{n-1} \frac{1}{\alpha_j}} = \frac{1}{n!}$  and

$1 + \sum_{j=1}^{n-1} \frac{1}{\alpha_j} = 2!(n-1)$ , as the below form.

$$\alpha_{n-2}^n = \frac{\binom{2(n-1)}{n!}}{\prod_{v=1}^{n-3} \alpha_v} \tag{A3}$$

Using the third equality in Eq. (18),  $\frac{\sum_{j=1}^{n-2} \alpha_j}{1 + \sum_{j=1}^{n-1} \frac{1}{\alpha_j}} = \frac{1}{3!}$ , as well as, Eqs. (A2) and

(A3), one can calculate the coefficients for the methods with  $n = 2, 3$ , and 4, easily. For other values of  $n$ , the authors utilized a heuristic procedure, which performs in an iterative manner shown in Figure A1. In this procedure, the coefficients  $\alpha_j^n$  are calculated using the coefficients  $\alpha_j^{n-1}$ . In order to stop iterations, the error introduced by Eq. (A4) should be computed at the end of each iteration.

$$Err = \sqrt{\sum_{k=1}^n \left( \frac{1}{k!} - R_k \right)^2} \quad (A4)$$

$$R_k = \begin{cases} \frac{1 + \sum_{j=1}^{n-1} \frac{1}{\alpha_j^{n,itr}}}{1 + \sum_{j=1}^{n-1} \frac{1}{\alpha_j^{n,itr}}} & k=1 \\ \frac{n-1}{1 + \sum_{j=1}^{n-1} \frac{1}{\alpha_j^{n,itr}}} & k=2 \\ \frac{\sum_{j=1}^{n-(k-1)} \prod_{v=0}^{k-3} \alpha_{j+v}^{n,itr}}{1 + \sum_{j=1}^{n-1} \frac{1}{\alpha_j^{n,itr}}} & k \geq 3 \end{cases} \quad (A5)$$

The error calculated by Eq. (A4) demonstrates the difference between the term on the left side of each equality in Eq. (18), which is estimated by the values of  $\alpha_j^{n,itr}$ , and the term on the right side of the equality.  $\alpha_j^{n,itr}$  is indeed the estimated value of  $\alpha_j^n$  in the iteration  $itr$ .  $\varepsilon$ , which is used to stop the iterations, has a very tiny value of  $1 \times 10^{-13}$ .

Figure A2 shows the values of  $Err$  obtained in calculating the coefficients  $\alpha_j^n$  for  $n=1$  to 100. The Results shown in Figure A2 illustrate the high ability of the authors' heuristic procedure in the calculation of  $\alpha_j$  in a wide range of  $n$ .

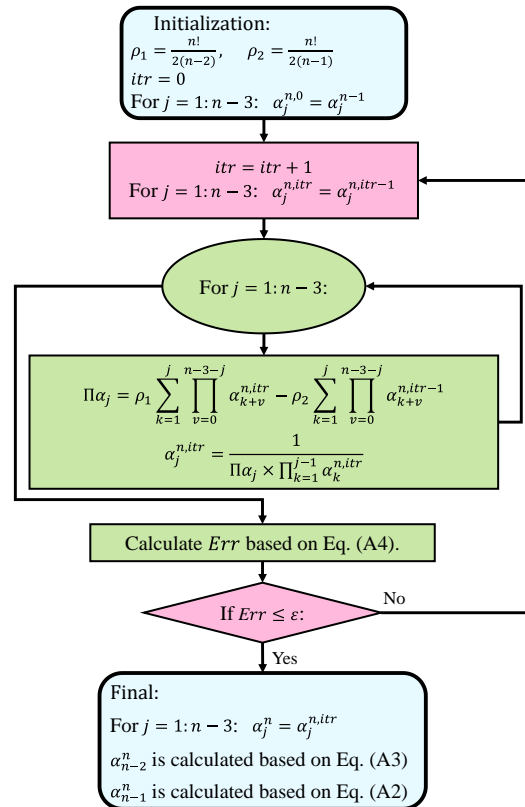


Fig. A1. The procedure for calculation of  $\alpha_j^n$  for  $n \geq 5$

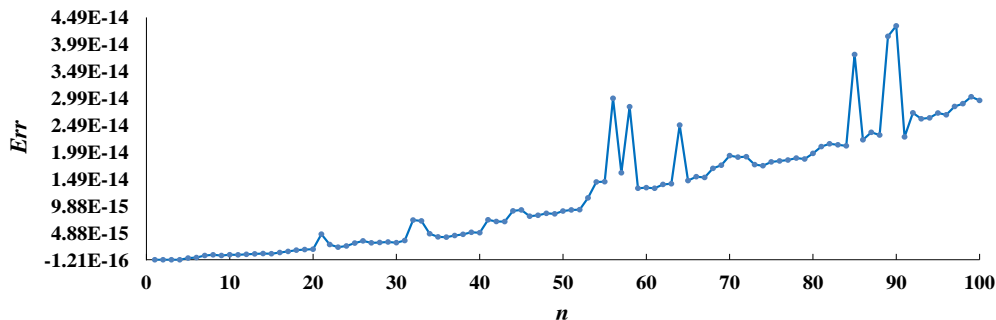


Fig. A2.  $Err$  for various values of  $n$